Instituto Tecnológico y de Estudios Superiores de Monterrey

Campus Monterrey

School of Engineering and Sciences

Investigation of the adhesion of MWCNTs on Inconel 718 metallic powders for their potential use in the development of aerospace applications.

A thesis presented by

Engr. Eduardo Bernales Soto

Advisor:
Dr. Alex Elías Zúñiga

Co-Advisor:
Dr. Nicolás Antonio Ulloa Castillo

Submitted to the
School of Engineering and Sciences
in partial fulfillment of the requirements for the degree of

Master of Science

In

Nanotechnology

Monterrey Nuevo León, December 10th, 2019

Instituto Tecnológico y de Estudios Superiores de Monterrey

Campus Monterrey

School of Engineering and Sciences

The committee members, hereby, certify that have read the thesis presented by Eduardo Bernales Soto and that it is fully adequate in scope and quality as a partial requirement for the degree of Master of Science in Nanotechnology.

Dr. Alex Elías Zúñiga
Tecnológico de Monterrey
School of Engineering and Sciences
Principal Advisor

Dr. Nicolás Antonio Ulloa Castillo
Tecnológico de Monterrey
Co-advisor

Tecnológico
de Monterrey
1 0 DIC 2019
Dirección Nacional de Posgrado
Dr. Rubén Morales Menéndez

Dr. Oscar Martínez Romero
Tecnológico de Monterrey
Committee Member

Dr. Daniel Olvera Trejo
Tecnológico de Monterrey
Committee Member

Dr. Rubén Morales Menéndez
Dean of Graduate Studies
School of Engineering and Sciences

Monterrey Nuevo León, December 10th, 2019

Declaration of Authorship

I, Eduardo Bernales Soto, declare that this thesis titled, “Investigation of the adhesion of MWCNTs on Inconel 718 metallic powders for their potential use in the development of aerospace applications” and the work presented in it are my own. I confirm that:

- This work was done wholly or mainly while in candidature for a research degree at this University.
- Where any part of this thesis has previously been submitted for a degree or any other qualification at this University or any other institution, this has been clearly stated.
- Where I have consulted the published work of others, this is always clearly attributed.
- Where I have quoted from the work of others, the source is always given. With the exception of such quotations, this thesis is entirely my own work.
- I have acknowledged all main sources of help.
- Where the thesis is based on work done by myself jointly with others, I have made clear exactly what was done by others and what I have contributed myself.

Eduardo Bernales Soto
Monterrey Nuevo León, December 10th, 2019

Dedication

For my mother, grandmother, family and Salma, the love of my life. Thanks to them I had the courage to pass my limits and have another vision of my life. For all your unconditional trust, support, patience, and encouragement: Thank you!

Acknowledgements

I would like to express my deepest gratitude to Dr. Alex Elías Zúñiga for all the support he gave me since I entered to study this master's degree and to my co-advisor Dr. Nicolás Ulloa Castillo who from the beginning was there providing me with the necessary help to develop my skills .

Finally, all of these wouldn't be possible without the sponsorship granted by Tecnológico de Monterrey through the Research Group of Nanotechnology for Devices Design, and by the Consejo Nacional de Ciencia y Tecnología de México (Conacyt), Project Numbers 242269, 255837, 296176, National Lab in Additive Manufacturing, 3D Digitizing and Computed Tomography (MADiT) LN299129 and FODECYT-296176. These institutions believed in my potential as a professional and researcher.

Investigation of the adhesion of MWCNTs on Inconel 718 metallic powders for their potential use in the development of aerospace applications

by

Eduardo Bernales Soto

Abstract

This research work focuses on studying the adhesion of Multi-Walled Carbon Nanotubes (MWCNT) to Inconel 718 metallic powders to enhance its physical properties. The adhesion of functionalized MWCNTs to the surface of the Inconel 718 metallic powders was carried out by drip incorporation. Experimental results by X-ray Diffraction (XRD), Fourier transform infrared (FT-IR), Thermogravimetric Analysis (TGA), and Scanning Electron Microscopy (SEM) provide evidence that the process followed to adhere the MWCNTs to the metallic powders was successfully achieved.

List of figures.

Fig 1 Ferrous Microstructure example. Adapted from [20] 14
Fig 2 Microstructure of Inconel 718 17
Fig 3 Body Centered Tetragonal atomic arrangement. 22
Fig 4 Face Center Face atomic arrangement 22
Fig 5 Internal parts of a turbine. 24
Fig 6 Pyramidalization angles present in different molecular structures [51]. 26
Fig 7 Graphene leaves a) Pristina, b) Hydrogenated and c) Stressed 27
Fig 8 Representation of MWCNTs. 29
Fig 9 Oxidation of alkenes by potassium permanganate (KmnO4). 31
Fig 10 Oxidation of alkenes by ozone followed by hydrogen peroxide. 32
Fig 11 Oxidation of alkenes by hydration of alkenes. 32
Fig 12 Formation of covalent bonds C-F. 33
Fig 13 Scheme of chemical modification of carbon nanotubes by acid treatment for anchoring carboxyl groups – adapted from [86]. 33
Fig 14 Fe3O4 coated with citric acid – Adapted from [88]. 34
Fig 15 Representation of citric acid coating metal oxide surface, adapted from [92]. 35
Fig 16 Fabrication procedures for CNTs/Al composite powder – Adapted from [45]. 36
Fig 17 FE-SEM of CNT/Al powders. (a) CNT clusters in untreated Al powders, (b)-(c) uniform adsorption of CNTs achieved by Al-PVA powders. Adapted from [45]. 36
Fig 18 (a) A schematic of GOCIP synthesis process and (b) the possibility of GOCIP bonding mechanism – Adapted from [95]. 37
Fig 19 Particle size distributions of nickel powders for different milling times, adapted from [98]. 38
Fig 20 Evolution of morphology in aluminum matrix. Adapted from [100]. 39
Fig 21 CNTs in aluminum matrix. Adapted from [100]. 39
Fig 22 Inconel 718 Powder. 41
Fig 23 MWCNTs structure. 41
Fig 24 Citric Acid ($C6H8O7$). 42
Fig 25 Parafilm. 42
Fig 26 Acids used A) Sulfuric Acid (H2SO4), B) Nitric Acid (HNO3) 42
Fig 27 Characterization by SEM of Inconel 718 powder as received. 43
Fig 28 Characterization by EDS to know chemical composition of Inconel 718. 44
Fig 29 Characterization by XRD of Inconel 718 powder as received. 44
Fig 30 Characterization by FTIR of Inconel 718 as received. 45
Fig 31 Characterization by SEM of MWCNTs as received. 46
Fig 32 Characterization by XRD of MWCNTs as received. 46
Fig 33 Characterization by TGA of MWCNTs as received. 47
Fig 34 Characterization by TGA of Citric Acid as received. 47
Fig 35 Characterization by FTIR of Citric Acid as received. 48
Fig 36 Diagram of the different process routes. 49
Fig 37 Weighted Inconel 718 and balls in closed containers. 51
Fig 38 Sealed Jar with Inconel 718 and the balls inside. 52
Fig 39 Fixed Jar in the mill. 53
Fig 40 Moment just before the sieving process. 53
Fig 41 Planetary ball mill. 54
Fig 42 Vibratory sieve shaker and sieves. 54
Fig 43 Atmos bag glove Bag with zipper-lock closure by Sigma-Aldrich. 55
Fig 44 Functionalized MWCNTs. 56
Fig 45 Functionalized Inconel 718. 57
Fig 46 Phase differentiation between Inconel 718 and MWCNTs. 57

Fig 47 Magnetic Stirrer and hot plate. 58
Fig 48 Ultrasonic Bath. 58
Fig 49 Particle size distribution of Semi-spherical morphology. 59
Fig 50 Particle size distribution of flake morphology 59
Fig 51 Semi-Spherical morphology by SEM. 60
Fig 52 Flake morphology by SEM. 61
Fig 53 Semi-spherical morphology with citric acid by SEM. 62
Fig 54 Semi-spherical morphology with citric acid by XRD. 62
Fig 55 Semi-spherical morphology with citric acid by FTIR. 63
Fig 56 Flake morphology with citric acid by SEM. 63
Fig 57 Flake morphology with citric acid by FTIR. 64
Fig 58 MWCNTs functionalized and seen through SEM. 65
Fig 59 MWCNTs functionalized and seen through XRD. 65
Fig 60 MWCNTs functionalized and seen through FTIR. 66
Fig 61 Semi-spherical morphology with MWNCTs by SEM. 66
Fig 62 Semi-spherical morphology with MWNCTs by XRD. 67
Fig 63 Flake morphology with MWNCTs by SEM. 67
Fig 64 Flake morphology with MWNCTs by XRD. 68

List of tables.

Table 1 Ferrous materials according to the application adapted from [20]. 16
Table 2 Types of non-ferrous metals [22]. 16
Table 3 Characteristics of the advanced materials trend adapted from [32]. 19
Table 4 Physicochemical properties of Inconel 718 21
Table 5 Chemical composition of Inconel 718 21
Table 6 Experimental design and processing routes. 50

Table of Contents

Abstract *6*

1. Chapter 1: Introduction and State of the art *11*

1.1. Motivation 11

1.2. Ferrous and Non-Ferrous Metals 12

1.2.1 Types of Ferrous Metals 13
1.2.2 Types of non-ferrous Metals 16
1.2.3 Trend of advanced materials 18
1.2.4 Super alloy Inconel 718 19

1.3 Carbon allotropes 25

1.3.1 Fullerenes 25
1.3.2 Graphenes 26
1.3.3 Carbon Nanotubes 27
1.3.4 Single-wall Carbon Nanotubes 28
1.3.5 Double-Wall Carbon Nanotubes 28
1.3.6 Multi-wall Carbon Nanotubes 29

1.4 MWCNTs/Inconel 718 Nanocomposite 30

1.4.3 CNTs oxidation 31
1.4.4 Metal-Matrix Functionalization 33
1.4.5 Adhesion and dispersion of CNTs in a Metal-matrix. 36
1.4.6 Morphology and adsorption capacity in a Metal-Matrix nanocomposite 37

2 Chapter 2: Objectives and Hypothesis *40*

2.1 General Objectives 40

2.2 Specific Objectives 40

2.3 Hypothesis 40

3 Chapter 3: Experimental Methodology and Results *41*

3.1 Materials 41

3.1.1 Main Rough Materials, characterization 42

3.2 Processing experimental routes 47

3.3 Ball-Milling process 51

3.3.1 Procedure 51
3.3.2 Equipment 54

3.4 Inconel 718 + MWCNTs: Chemical functionalization process 55

3.4.1 Procedure 55
3.4.2 Equipment 58

3.5 Size statistic 59

4.5.1 Semi-Spherical Morphology 59
4.5.2 Flake Morphology 59

4 Chapter 4: Results and Discussions *60*

4.1 Ball milling Process 60

4.1.1 Semi-Spherical Morphology 60
4.1.2 Flake Morphology 61

4.2 Functionalization of Inconel 718 62
4.2.1 Inconel 718 Semi-Spherical with Citric Acid 62
4.2.2 Inconel 718 Flake with Citric Acid 63
4.3 Functionalization of MWCNTs 64
4.4 Adhesion of MWCNTs in Inconel 718 66
4.4.1 Inconel 718 Semi-Spherical 66
4.4.2 Inconel 718 Flake 67
5 Chapter 5: Conclusions 69
5.1 Conclusions 69
References 70

1. Chapter 1: Introduction and State of the art

1.1. Motivation

In the last decades, there has been an exhaustive effort to investigate advanced materials with improved properties as it is mechanical, electrical or thermodynamic performance. An important requirement to develop such advanced materials is that they must be manufactured in a relatively easy way. In the aerospace area, the improvement of existing materials is a part that has a great focus [1]. This is due to the fact that continuous development is needed to avoid major failures in the different parts that make up an aircraft.

It is because of this that advanced materials arise which are a key element in industrial innovation. These are developed as materials with new properties and better performance, which allow to obtain more competitive, safe, efficient products. The importance of advanced materials in the industrial sector is that they provide production technologies that are aimed at developing cheaper products, with better performance, more durable and with greater added value [2].

These materials have impacted different techniques within the sector and have had an important development in fusion technologies and metal transformation, powder metallurgy, synthesis technologies and advanced ceramics manufacturing., Composite materials of metallic, ceramic and organic matrix, surface technologies and joining technologies. However, there are challenges that they face in the future, which range from improving the performance of current materials to increasingly demanding service actions, reducing the cost of products without reducing their characteristics, more effective new coatings and durable, joining methods between more reliable and versatile materials [3].

Given the implications of these advanced materials, the need to improve existing materials in the different components of an aircraft. Since this gives possibility to create mechanically more stable aircraft in its different phases. Also, in literature many experimental studies explore the possibility of increasing the junction temperature limit, beyond the limits established by manufacturers, in order to increase power capabilities. [4].

These improvements can be made through advanced materials which have been used in parts of the turbine for several years. However, the trend points to something even more viable, which are the nanocomposites, since these being modified from the base structure of the material, leads to raising specific properties that are required [5].

Given the hardness of some metal alloys, it is very difficult to manufacture parts or prototypes, the above has motivated the implementation of new technologies that allow manufacturing more efficiently. It is the reason why material modifications are currently being implemented from their base (nanocomposites) through new manufacturing techniques. A clear commercial method of manufacturing alloy metal powders is atomization, in recent years and coinciding with the development of metal matrix composite materials (MMC), processes based on grinding are emerging as an effective method to achieve, both alloys difficult to obtain by other methods such as composite powders [6].

Of all of them, one of the most effective and of most interest is the mechanical alloy. Mechanization and chemical bonding have proven to be the most favorable technique for obtaining nanocomposites pre-alloyed powders, due to the possibility of a good control of the chemical composition, size, shape and granulometric distribution thereof. These characteristics, important for subsequent compaction, added to the possibility of obtaining a fine microstructure with a high solute content, have made atomization the process of obtaining dust with greater industrial implantation [7].

Against this, the mechanical alloy is the most current mechanical process for obtaining dust, by allowing compositions and levels of properties impossible to achieve by other methods, including atomization. This technique was first studied and developed in the mid-1960s, by John S. Benjamin, which consists of an effort to find a way to combine the hardening by dispersion of oxides with the hardening by precipitation of nickel-based superalloys for applications in gas turbines [8]. Since then, mechanical alloy has diversified its scope from iron-based alloys to aluminum alloys and ceramic systems and is already marketing numerous materials. Defined as a dry grinding process, the fundamental advantage it presents is precisely the possibility of obtaining unattainable compositions by processes such as atomization, raising the solute content well above the equilibrium compositions and increasing the percentage in reinforcements, eliminating the problems of segregation and formation of agglomerates generally associated with conventional powder metallurgical mixtures [9].

The review in the literature indicates that similar methods have been used over time, but that in order to streamline current processes, it is necessary to implement techniques that yield nanocomposites that can be carried through additive manufacturing. These nanocomposites should have as a principle at least stronger chemical interactions that help create an increase in their properties and that as a final result when applied in the industry show a greater ease of being machined [10].

1.2. Ferrous and Non-Ferrous Metals

There are materials that are currently used in different industrial sectors such as: aerospace, motor, electrical. These materials are classified according to their composition, properties, and applications. But there are two types that especially have enough relevance and multiple applications for many years, these are ferrous and non-ferrous materials [11]. In order to make and understand the study carried out, a thorough investigation of these two types of materials was made and thus be able to give a result of why the material to be studied is better or may have a greater range of application.

Starting with non-ferrous materials it is remarkable to say that they are made of iron its alloys, sweet or wrought iron, steel and cast iron. They are the most used due to their low cost of extraction and obtaining. Iron is the chemical element (Fe) that constitutes 5% of the earth's crust (2nd most abundant metal). It is not present in its pure state but in combination with other elements in minerals: magnetite, siderite and hematite. Its main drawback is that it can oxidize by reacting with oxygen from the air or water by degrading the metal until it causes it to break [12].

The distinctive attribute of iron is that it is dense, strong when mixed with carbon, abundant and easy to refine, highly susceptible to corrosion and magnetic. Making iron alloy with other elements in different proportions can mitigate or eliminate one or more of these factors [13].

Ferrous alloys with carbon are usually called iron or steel, and can contain any number of other elements, from aluminum to vanadium, based on their specifications. These metals are usually chosen for their mechanical properties. Multiple investigations are focused on its elastic limit, hardness, ductility, weldability, elasticity, ease of cutting and thermal expansion, which describe how a material will behave under specific stressors. In ferrous metals, iron and steel are the most common foundry materials [14].

1.2.1 Types of Ferrous Metals

It is necessary to emphasize that there are different types of ferrous materials, some with better properties over others, this depends on what application is given. A notable example is cast iron which is a category of iron alloys with carbon content greater than 2%. They are relatively cheap and dense irons. When they are heated and melted, they have much greater fluidity at lower temperatures than steel, this means that they can flow inwards and fill the parts of a complex mold with greater efficiency. Cast iron also shrinks at half the rate of steel while cooling [15].

The applications of ferrous metals are multiple, starting with the applications of iron, which in itself does not have many applications, these can be highlighted: electromagnets and as a starting material for moldable cast iron, since that is a soft material. Ferrous materials have a lot of uses, they can be differentiated between them: in the construction it is used in a multitude of elements from rods, bars to palastros, beams and slabs; in the shipping industry they are used for their characteristics of armed and salinity resistance, in some of their variations; military industry, its main use in this field are weapons for their resistance to high temperatures and the environment; In the automobile industry, it was used in the seventies, today its use in this field is almost nil and in the food industry stainless steel is used in the manufacture of machinery for its resistance to liquids and for the absence of microbes on the smooth surface of this material [16].

Foundries are mainly used in the manufacture of parts because they are easy to machine and mold. They are very resistant to mechanical stress and good compression properties, but they are fragile: they will break before bending or distorting. This vulnerability may mean that the fragile grades of cast iron are not used for designs with extruded or elaborated details, or with sharp edges, since these characteristics can be chopped [17]. That is why it is very important to know the microstructure of the ferrous material that is had, since this will determine many of the intrinsic properties of the material.

These challenges mean that steel can be much more intense than working to mold it well. He requires expert attention during all stages of his production. Even so, the high mechanical strength of the final product can make a steel alloy the clear choice for some applications, with the machining providing final stage finishes [18].

Pure iron has very few technical applications because its properties are very poor. But combine it with small amounts of carbon, a nonmetal, greatly improves its properties depending on the amount of carbon added to iron. For example, it is notorious to distinguish the following alloy: mild iron, steels, and smelters [19]. A clear example is the ferrous of what an alloy of this type looks like, which can be a starting point for determining different mechanical, chemical and metal composition properties is the microstructure of G10100 steel sheet (Figure 1).

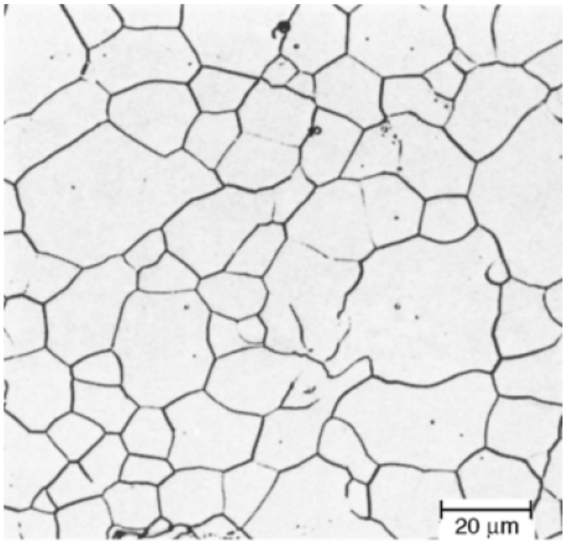

Fig 1 Ferrous Microstructure example. Adapted from [20]

There is also another way to classify this type of ferrous materials, this is due to the adhesion of carbon, since the adhesion of this provides properties to the material. Due to this, the range of application may increase, this is expressed in table 1.

Material	Characteristic	Properties	Applications

Wrought iron	Carbon content less than 0.03%.	·It oxidizes easily and cracks internally. ·Soft, the purer. ·Ductile and malleable. ·Good conductor of electricity. ·Supports the forge to mold it. ·Difficult welding.	Electrical applications. Electromagnets cores.
Steels	Carbon content between 0.03% - 1.76%.	·Excellent mechanical properties: hardness, toughness, stress resistance. ·The harder the more carbon. Under cost of obtaining. ·They oxidize easily. ·They allow good welding. ·They admit forging and machining.	Tools, nails, screws, watches, rail vehicles, cars, boats, beam profiles. Machinery, cutting, surgical equipment, space vehicles, nuclear reactors
Foundries	Carbon content between 1.76% - 6.67%	·Less ductile and less stubborn than steels. ·Bad weld. ·Harder than steels since carbon gives it hardness but increases fragility. ·Easier to machine than steels.	Lampposts, benches, fountains, sewer covers. Benches or blocks of engines, machinery, boilers, ingots to obtain steel.

		·They melt easily, the lower temperature than steels and pure iron (400ºC less). ·They allow obtaining pieces of different complexity and size using molds.	

Table 1 Ferrous materials according to the application adapted from [21].

1.2.2 Types of non-ferrous Metals

Comparing ferrous materials with non-ferrous materials, it can be seen that non-ferrous materials, their applications are more specific, however, since they are non-ferrous materials, it does not mean that there is no iron in their composition, it may be existing but it is not their majority base. Taking into account the most used, and with more range was applied, the most important are 7: Copper, Zinc, Lead, Tin, Aluminum, Nickel and Manganese. There are many other non-ferrous metals; However, since the quantities produced are small, or the processes are highly expensive, they are rarely used [22]. They are classified according to their density in heavy, light and ultralight. Table 2 shows the types, their characteristics and the existing metals.

Types	Characteristics	Metals
Heavy	Its density is equal to or greater than 5 kg / dm3	Tin, Copper, Zinc, Lead, Chrome, Nickel, Tungsten or Tungsten and Cobalt.
Light	Its density is between 2 and 5 kg / dm3	Aluminum, Titanium
Ultralight	Its density is less than 2 kg / dm3	Magnesium

Table 2 Types of non-ferrous metals [23].

Each of these classifications have different applications, however, there are alloys between these materials that can give a higher range of properties and applications. But if we take into account non-ferrous materials alone, they have characteristics such as: Soft, high corrosion resistance (higher than ferrous alloys, high electrical and thermal conductivity, low density, ease of production. That’s why non-ferrous materials are used in manufacturing as complementary elements of ferrous metals, they are also very useful as pure or alloyed materials which, due to their physical and engineering properties, cover certain requirements or working conditions, for example bronze (copper- tin) and brass (copper-zinc) [24].

Therefore, to improve their properties, they are usually alloyed with many more metals. For example, the alloy of Inconel 718, which being an alloy reinforces its properties. Looking at the microstructure (Figure 2), It is possible to know which phases exist mostly, which will give them such unique properties.

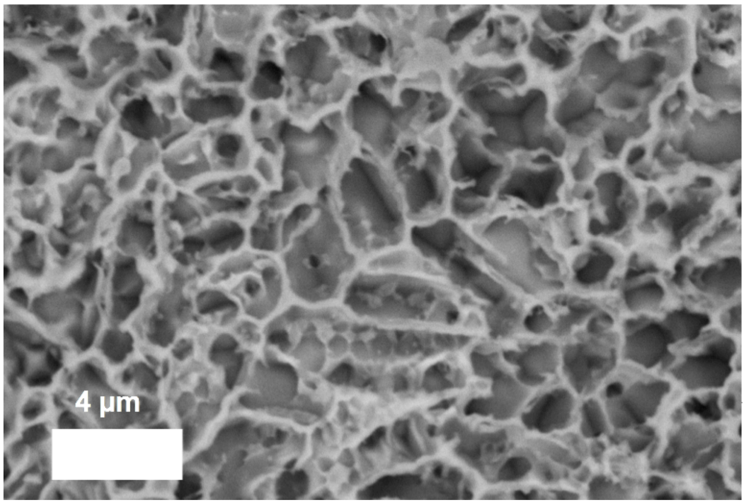

Fig 2 Microstructure of Inconel 718

Even when the characteristics are marked in this way, it is not possible to generalize, because each of them can have a completely different property and application. An example of them is aluminum which is a silvery and shiny white metal in a state of high purity, it is quite ductile and malleable compared to its weight it is quite resistant mechanically, it has high thermal conductivity. In its natural state it is found in many silicates (feldspar, plagioclase and micas) [25].

But if we look at another type of non-ferrous material that is highly used, it encounters copper which is a red metal, very malleable ductile state of high purity, has a high thermal and electrical conductivity, copper in normal atmospheric conditions is quite resistant to corrosion, but when the temperature is wet it is discovered with a layer Green jade platinum or cardinal that protects them from further attacks.
Due to its high electrical conductivity, ductility and malleability, it has become the most used material to manufacture electrical cables and other electrical and electronic components [26].

Placing one of the non-ferrous materials used strongly in the aerospace sector, is the nickel and its alloys, this is because the nickel is hard and very stubborn when it contains a small amount of Carbon, it becomes malleable, leaving small amounts of magnesium laminated, very resistant to atmospheric corrosion, and allied to iron it imparts great oxidation resistance. These alloys are used to make coins, jewelry, and items such as valves and heat exchangers. Most of the nickel is used to make stainless steel [27].

It can also be combined with other elements, such as Chlorine, Sulfur and Oxygen to form nickel compounds. Many nickel compounds dissolve easily in water and are green in color. Nickel compounds are used in nickel plating, to color ceramics, to make batteries and as catalysts, which are substances that accelerate chemical reactions [28].

Highlighting ferrous and non-ferrous materials as materials that are already used today, it is necessary to know where they are going and how they plan to apply in the future. This is why advanced materials arise, which are conjunctions of ferrous and non-ferrous materials.

1.2.3 Trend of advanced materials

Advanced materials are found within the entire spectrum of types of materials and can be classified as: metallic materials, high performance polymers, advanced ceramic materials, composites and biomaterials. These materials show superior mechanical characteristics of strength, hardness, toughness and durability in relation to conventional materials [29].

The advanced materials production technologies are aimed at developing cheaper products, with better performance, more durable and with greater added value.

OBJECTIVES – CHARACTERISTICS	EXAMPLES OF DEVELOPED PRODUCTS
Superior mechanical properties, including toughness, fatigue resistance and wear resistance.	Low alloy steels, economical, with very high strength and deformability, to increase the safety of cars and transport in general.
Use of durable coatings to achieve the required surface properties without altering the characteristics of the original base material.	Light alloys and composite materials for the automotive and aeronautical sectors.
Specific surface treatments (chemical and mechanical) to increase the performance of the products and maximize their durability.	Alloys and coatings resistant to high temperatures, to the action of very aggressive environments and with a greater tolerance to damage.
Complex on-demand microstructure design to maximize the performance of industrial components.	New steels for higher performance rail, which ensure greater durability before increasing service loads.

Materials to work in extreme environments (high and low temperatures, very corrosive environments).	Tenacious ceramics capable of supporting with sufficient reliability mechanical and thermal loads.
Materials with new functionalities and better performance throughout its useful life.	New coatings resistant to corrosion and wear.
Light and sustainable materials for the automotive industry and for the aerospace industry.	New materials easy to be machined and still with high mechanical properties.

Table 3 Characteristics of the advanced materials trend adapted from [29].

Some of the challenges that will be taken for the future is to be able to provide materials that increase the parameters that the system has. A clear example is aerospace ships, which could be faster if the composite material in its turbine withstood a higher temperature.

This is something that is already being carried out in experimentation phases, a sample of this are the advanced compounds based on titanium / aluminum and carbon fiber, which generate a material 3 times more resistant to steel, maintaining at a time, a considerable support for high temperatures [30].

One of the materials that is rising in its applications and that are being considered strongly are super alloys, since they show excellent mechanical and creep resistance (tendency of solids to move slowly or deform under tension), resistance to high temperatures, stability and high resistance to corrosion and oxidation. Much of these properties are the nickel super alloy, the so-called Inconel 718.

1.2.4 Super alloy Inconel 718

The Inconel 718 is a material that began to be developed in the mid-twentieth century and used profusely since the 60s for the manufacture of aeronautical engine components among other things, and that is still used today in many reactor components. This is not an obstacle for further research into the evolution of this alloy by the material departments of companies in the sector or the introduction of new ones with improved properties [31].

Nickel-based alloys operate in the components of an aeronautical gas turbine at temperatures as high as 80-85% of their melting temperature, which makes it necessary in certain areas to use aids such as internal cooling of the blades themselves by means of micro holes arranged for this purpose, or the use of ceramic thermal barriers to allow a high operating temperature and thus maintain the efficiency of the motors. This thermodynamic efficiency of the thrusters is, as is known, the higher the higher its operating temperature, and at this point the current state of the art meets the maximum physical temperature limit bearable by the materials of the components that integrate the motor [32].

This is the trend of current research in this type of materials, to find the right key to achieve a new superalloy that allows maintaining the level of properties of mechanical resistance, corrosion resistance, creep resistance. at a higher operating temperature of the components.

One of the great challenges in the metalworking industry is to get the perfect, valid tool to machine any material that comes your way. This impossible today, does not prevent the tooling industry from being a constantly evolving industry, to which new challenges are presented every day in the form of new materials to be machined or evolutions of those that already existed [33]. With a lot of security in the metalworking industry, the families of the most demanding materials for machining are super alloys. These characteristics may be related to its poor thermal conductivity, chemical affinity with the tool, ductility, or presence of abrasive particles, for example, which constitute important threats to perform quality machining.

Among these materials are super alloys, which have had a high impact of applications in the automotive, aerospace, metallurgical and environments where properties exceed existing alloys. Among the most applicable and with good properties is the super alloy Inconel 718. This is a nickel-base superalloy largely used in the fabrication of critical pieces for turbine engines because of its high mechanical properties (yield strength up to 650ºC, impact strength and fracture toughness down to -40ºC), as well as good corrosion resistance. In addition, this alloy can be easily forged and welded.[34]

Its superior mechanical properties and its resistance to high temperatures and to corrosion have led to its extensively used as a structural material in a wide variety of applications in the aerospace industry, such as disks, blades and shafts in gas turbine engines, where a high level of strength under high-temperature conditions is an important design consideration. [35]

The great impact and application of Inconel 718 is reflected in its physicochemical properties, which can be applicable in different fields and can be modified if a nanocomposite is created. The most important properties of Inconel 718 are shown in table 4.

	Property	**Value**
Electrical	Electrical Resistivity	125 µOhmcm
Physical	Density	8,19 g cm^{-3}
	Melting Point	1533.15- 1608.15 K
Magnetic	Initial permeability	1,0013
	Curie temperature	<- 469.15 K
Mechanical	Elongation	<15 %

	Brinell hardness	250-410
	Elasticity Module	200 Gpa
	Tensile Strength	800-1360 Mpa
Thermal	Specific Heat at 23C	435 J K^{-1} kg^{-1}
	Thermal Expansion Coefficient	13,0 x10^{-6} K^{-1}
	Thermal Conductivity at 23C	11,2 W m^{-1} K^{-1}
	Maximum Air Use Temperature	973.15 K

Table 4 Physicochemical properties of Inconel 718

Inconel alloys belong to the Ni–Cr based superalloys family which cover a wide range of compositions and mechanical properties. Ni and Cr provide resistance to corrosion, oxidation, carburizing and other damage mechanism acting at high temperature. Inconel alloys have good cryogenic properties, good fatigue and mechanical strength at moderate temperatures and relatively good creep behavior. Usually, Inconel alloys are extra-alloyed with Al, Ti, Nb, Co, Cu and W to increase mechanical and corrosion resistance. Fe can also be present in amounts ranging 1–20%. These superalloys are indented for heat treatment recipients, turbines, aviation, nuclear power plants, and so on. [36] The Inconel 718 is composed of the elements described in table 2 [34].

Element	Percentage
Ni	53
Cr	19.06
Fe	18.15
Nb	5.08
Mo	3.04
Ti	0.93
Al	0.52
Co	0.11
C	0.021
Cu	0.02

Table 5 Chemical composition of Inconel 718

The strengthening phase in the alloy 718 is the metastable body centered tetragonal Ni_3Nb (DO_{22}) γ'' phase [34] (shown in Fig 3).

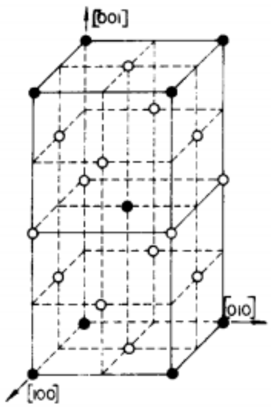

Fig 3 Body Centered Tetragonal atomic arrangement.

Also, the existence of a small amount of a γ' phase Ni_3(Ti, Al) (shown in figure 4) (fcc $L1_2$ structure), appearing as a fine dispersion, of quasi-spherical particles which are coherent with the matrix. The role of the γ' phase is also strengthening, but to a lesser degree than the Inconel 718 is a nickel base superalloy largely used in γ'' precipitates (the volume fraction of γ'' is four times the manufacture of critical pieces for turbine engines be- bigger than that of γ') [37].

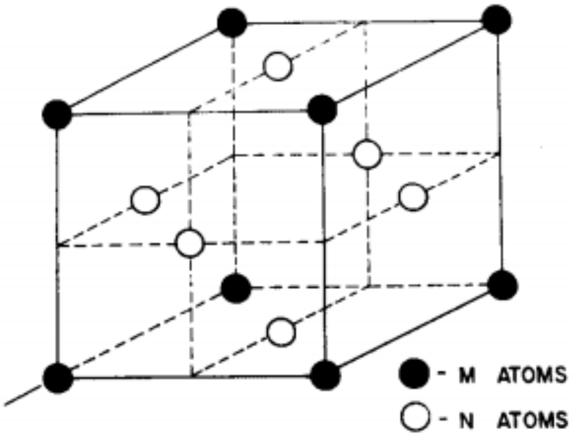

Fig 4 Face Center Face atomic arrangement

Taking into account its phases, properties and advantages, it is said that the family of superalloys constitutes one of the most demanding in terms of its metallurgy. These materials are generally Nickel-based alloys and have widespread use in the aeronautical sector due to their exceptional mechanical strength and toughness characteristics, as well as high corrosion resistance, all at high temperature. However, it is one of those that present a more difficult machining. This is why in recent years there have been numerous advances in the field of superalloys, both in terms of metallurgy and processing methods, especially in relation to its machining, both in techniques and tools [38].

These advances are the logical consequence of investment and continuous research in this type of materials by aircraft engines and smelters. Traditionally, a multitude of different components have been manufactured with this alloy, mainly for the hot zones of aeronautical engines, for their unmatched properties already mentioned, such as discs, housings, seals, spans, blades, etc. and until recent times there has not been much variation in this aspect [39]. But the new efficiency requirements of the new generation of aeronautical engines make the materials have to be able to withstand higher temperatures in service and therefore a new generation of materials with improved properties is necessary to allow these necessary increases in operating temperature [40]. That is why it is necessary to propose an improvement of Inconel 718 through a reinforcement, since the technologies currently applied do not allow to exceed that limit which would allow a wide range of application.

Currently, Inconel's approach to adhesion of carbon nanotube reinforcements throws the additive manufacturing (AM) this technology develops rapidly in the recent years, which has shown a large potential and annually growing market of manufacturing [41]. Among all the AM techniques, electron beam melting (EBM), selective laser melting (SLM) and selective laser sintering (SLS) are the most widely used AM processes, which can manufacture near-net-shape parts directly up to 99.9% relative density [42].

While it is necessary to provide a substantial amount of depositing powder in all of the powder bed AM methods mentioned above. To overcome this deficiency, laser powder deposition (LPD) is applied, which is also termed as laser metal deposition (LMD), laser cladding or laser deposition. Compared with the powder bed AM processes, LPD consumes a much lower amount of powder and in turn, provides much greater system flexibility to produce the additive layers as the depositing powder is fed and melted into the molten pool simultaneously through a coaxial or lateral nozzle during the deposition process. Therefore, it is proved to be more feasible for repair or remanufacturing, especially for the repair of high-valued nickel-base superalloy components [43,44].

1.2.4.1 CNTs in a Metal Matrix

The properties in CNTs-Metal compounds often deteriorate seriously with the increase in CNT content, especially when the CNT content is greater than 2% by volume, this problem is attributed to three reasons: first, it is very difficult to homogenize the dispersion of large quantities of CNT In the metal matrix , the strong interactions of Vander Waals generate agglomerations of CNT. Secondly, the specific surface area of CNT is so large that the interface / volume ratio is much larger than that of conventional matrix compounds, so that the properties are more sensitive to the interfacial bond, thirdly, porosity after consolidation and sintering [45].

It’s important to develop effective manufacturing methods that not only can disperse high-content CNT in the Inconel matrix, but can also achieve a good bond between the CNT and the metal matrix. Flake powder metallurgy has many advantages in disperse a high content of nano reinforcements evenly into metal nanoflakes.

The disk-shaped nano scales with dozens of microns in diameter and a few hundred nanometers thick have a greater CNT dispersal capacity than metal sphere particles. Also, there are a better dispersion of CNT by surface modification in both Metal matrix particles and carbon nanotubes, this functionalization of the surface leads to a strong bond and prevents regrouping during filtering and drying [46].

1.2.4.2 Areas of opportunity

To achieve successful manufacture of the nanocomposite, there are several barriers or areas of opportunity to overcome. We need conductive carbon nanotubes connected each other embedded in a metal matrix in a homogeneous way, also a metal matrix properly designed to maximize the good adhesion between the matrix and the nanotubes is required, [47]. Additionally, stable productions methods are required which prove nanotubes homogeneously dispersed in the matrix. Similarly, the cost of production must be low to allow the use of large quantities of carbon nanotubes [48].

Traditionally, a multitude of different components have been manufactured with Inconel 718, mainly for the hot zones of aeronautical engines, for their unmatched properties already mentioned, such as discs, housings, seals, spans and blades. And until recent times there has not been much variation in this aspect. But the new efficiency requirements of the new generation of aeronautical engines make the materials have to be able to withstand higher temperatures in service and therefore a new generation of materials with improved properties is necessary to allow these necessary increases in operating temperature [49].

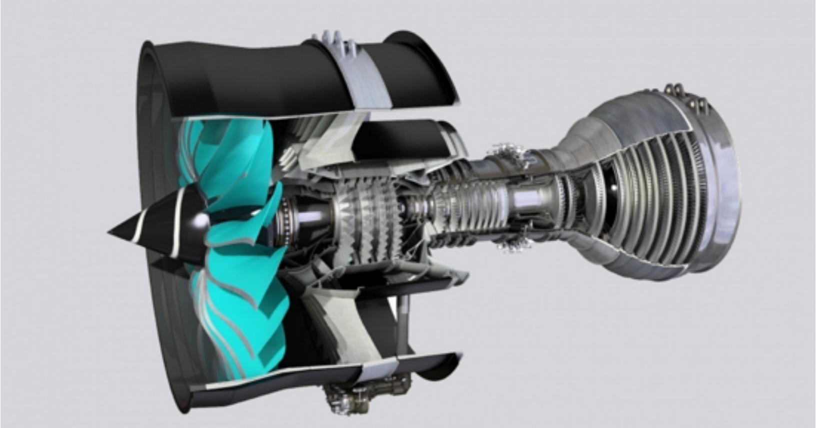

Fig 5 Internal parts of a turbine.

1.3 Carbon allotropes

The different carbon phases have been used for many years to add properties to metals and alloys, which without this adhesion would not be possible to have them. That is why it is very important to be able to study in depth the existing allotropies, since each one can add advantages or disadvantages when being added to metallic matrices. There are different carbon allotropes such as fullerenes, graphenes, carbon nanotubes have been investigated strongly lately [50].

1.3.1 Fullerenes

Fullerenes have had utility with metals, but mostly to encapsulation of them. That is why they took place in modern materials for nanoscience, as far as carbon-based materials are concerned. Since its discovery, fullerenes have been the focus of attention for the scientific community. The fullerene C_{60} is the most abundant and representative [51]. In the 18th century, the Swiss mathematician Leonhard Euler showed that a geodesic structure can contain 12 pentagons to become a spheroid, although the number of hexagons can vary. Fullerenes are represented by the expression C_n, where n represents the number of carbon atoms present in fullerene. Fullerenes are formed with an even number n ≥ 20 of three vertices, 3/2 edges and (- 20) / 2 hexagonal faces [52]. The icosahedral forms of the fullerenes lead to a concentration of curvature [53] (or pyramidalization in the carbon atoms) in the five-member rings, which begin to assume the role of vertexes in the fullerene in a polyhedral form [54]. This observation has implications for the reactivity of the fullerenes [55].

The pyramidalization angle θp is defined as $\theta p = \theta\sigma\pi - 90º$, where $\theta\sigma\pi$ is the angle between the π orbital and the σ bond of the C atom of interest [51]. For a carbon atom with hybridization sp^2 (trigonal), a planar structure is strongly preferred, this implies a pyramidalization angle $\theta_P = 0º$, whereas a hybridization sp^3 (tetrahedral) carbon atom requires $\theta_P = 19.5º$ (Figure 5). The atoms of C_{60} have $\theta_P = 11.6º$, it is clear that their most appropriate geometry would be Tetrahedral [56].

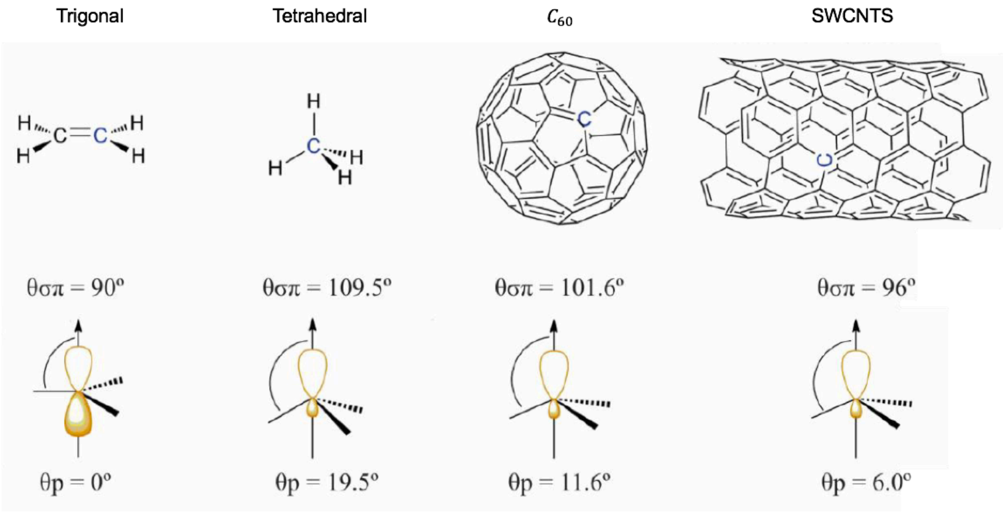

Fig 6 Pyramidalization angles present in different molecular structures [51].

This pyramidalization has been taken into account because it is a similar process that occurs in graphene sheets, forming forms such as SWCNTs. It is through this process that the use of fullerenes is in mind as a good possibility of being applied to metals not only encapsulating them, but also being able to play an important role in surface adhesion.

1.3.2 Graphenes

The technology industry has placed much of its hopes in graphene, because due to its structure and reactivity, when added to a metal matrix, graphene sheets play an important role in increasing their properties. This is because the graphene is a structure of carbon atoms that form a regular hexagonal pattern that are generated from hybrid sp^2 orbitals on carbon. The detailed reactivity of graphene sheets, in terms of size, shape and the possibility of a stoichiometric control, is still explored [57]. However, it can be expected that the royal selectivity based on zig-zag or arm-chair at the terminations in the graphene plane will manifest certain reactions. The formation of a covalent bond in the basal plane of the graphene sheet requires the breaking of sp^2 bonds and formation of sp^3 bonds [58]. An unpaired electron that is created in the place adjacent to the covalent attachment point improves the reactivity there, which leads to a chain reaction from the initial point of attack.

In addition, the principle of geometric stress minimization can establish reactivity. Figure 6 illustrates that the covalent bond between a hydrogen and carbon atom will cause atomic displacement of bonded carbon above the plane of the sheet, and this stress can be minimized by having a second hydrogen atom anchored to the opposite side of the leaf releasing tension.

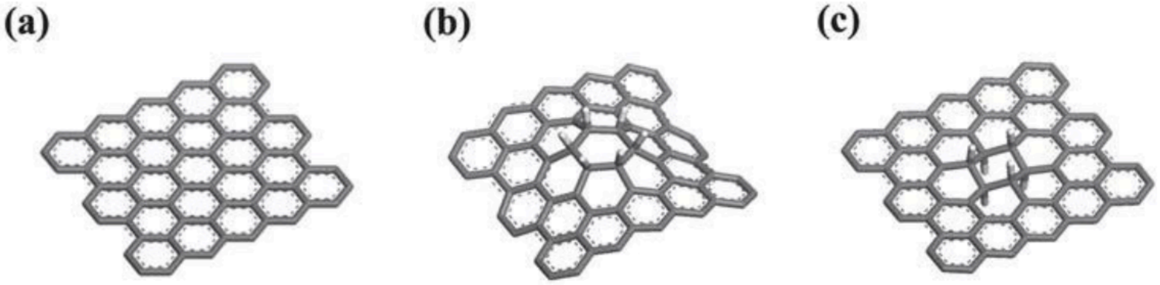

Fig 7 Graphene leaves a) Pristina, b) Hydrogenated and c) Stressed

The geometrically tense regions in the graphene network are areas of preferential reactivity due to the displacement of electrons above the plane. Due to the 2D nature of the graphene sheets, the edge regions play an important role in the electronic structure of the molecules. The edges can be manifested as a zig-zag or arm-chair. At the zigzag edges, the attainment of aromatic sextets is frustrated in most rings, therefore a structure of this type is thermodynamically unstable in comparison with the armchairs. It is then expected that the zigzag edges show greater reactivity compared to the armchairs [59].

This geometry is strongly used as an advantage when making an adhesion with some other material, since due to this versatility in its geometry it is possible to have different shapes within the same matrix, one transposed above another. This helps in principle that there is a greater connection between graphene sheet that speaks of a greater increase in electrical conductivity for example.

1.3.3 Carbon Nanotubes

The great limitation of carbon nanotubes (CNT) in practical applications is the great difficulty of manufacturing devices in which they are placed in a controlled and well aligned way. Today, several thousand tons of CNT are manufactured annually, but their utility is reduced to applications where they can be placed randomly and in large quantities.

As the synthesis, purification and chemical modification techniques of the CNT have advanced, they have been incorporated into thin film electronics and surface coatings. In these applications films are used in which the CNTs are messy, such as thread forests. The mechanical, thermal, and electrical properties of these CNT macrostructures are much lower than those of individual CNTs. But manipulating CNTs one by one at the industrial level is beyond current techniques.
This is due to the structure of the CNTS since it can be considered as a sheet of graphene rolled on itself [60]. Depending on the degree of winding, and the way in which the original sheet is formed, the result can lead to nanotubes of different diameter and internal geometry. These tubes shaped as if the ends of a paper were

joined at their ends forming a cylinder are called monolayer nanotubes. There are also nanotubes whose structure resembles that of a series of concentric tubes, including some within each other, of increasing thicknesses from the center to their surroundings. The latter are multilayer nanotubes. Generally, monolayer nanotubes have a diameter of approximately 0.7 to 10 nm and a length of the order of microns, so their ratio length / diameter is approximately $10^4 - 10^5$ and due to this is that they are considered one-dimensional structures (1D) [61].

1.3.4 Single-wall Carbon Nanotubes

In the industrial sector, the adhesion of SWCNTs in metal matrices for the reinforcement of metal has been experienced. However, being able to add SWCNTs is a complicated process, since producing them is only highly expensive. That combined with SWCNTs are very volatile, which makes them difficult to be handled and industrialized. When talking about them stably, this is an important factor since producing defects in them for a functionalization is more difficult and expensive because of their intrinsic stability.
Since these are formed of a cylinder and generated when a graphene sheet of a certain size is wrapped in a certain direction in such a way that two crystallographically equivalent sites of the hexagonal network coincide. An SWNT consists of two different regions with different physical and chemical properties. The first region is the graphene sheet that forms the wall of the tube and the second region is the lid (carbon atoms C placed in hexagons and pentagons form the structure) that covers the end of the tube. The cap of the tube sometimes has a structure similar to that of fullerene C_{60}, so that if the two caps were joined, they would generate a C_{60} molecule or another fullerene type [62].

1.3.5 Double-Wall Carbon Nanotubes

If SWCNTs turn out to be expensive to be applied in the industrial sector, the focus is on nanotubes with more walls. This is where the Double-wall Carbon Nanotubes (DWCNTs) come in, which, being double-walled, maintain a lower stability, making them more manageable, more optimal to be able to develop processes such as functionalization or simple adhesion. It is important to note that DWCNTs consist of two individual carbon nanotubes, with one embedded inside the other.
The differences in diameters and the chirality of the two different nanotubes lead to a varying degree of interaction between the two, while at the same time the properties of the individual nanotubes being separate from each other [63].

It is this wide variety of possibilities that have made DWCNTs a focus of interest for carbon nanotube research. Varying chirality allows a range of inner-wall outer-wall interactions to occur, because the chirality determines whether the nanotube will be semiconducting or metallic. It is possible to achieve metallic-metallic, semiconducting-metallic, metallic-semiconducting or semiconducting-semiconducting interactions. In addition to this, the metallic and semiconducting properties can vary depending upon the exact lattice parameters, which enables a wide range of possible property combinations [64].

DWCNTs also have a large advantage over single-walled carbon nanotubes, as it is possible to modify the outer nanotube without changing the properties of the inner nanotube. This modification could be either through functionalization (to add solubilizing groups), or the doping of the structure (to alter the properties). This allows the double-walled system to maintain functionality of a single-walled nanotube whilst simultaneously having the solubility of functionalized nanotubes.

1.3.6 Multi-wall Carbon Nanotubes

One of the most used in the industrial sector is the Multiwalled carbon nanotubes, this is because its multiple walls allow the nanotubes to have an instability that is used as an advantage so that they can be processed by different routes. Having multiple capable, contrary to what one might think, these are cheaper and more accessible to handle. It is the reason why they are taken into account to be added in different metal alloys to increase some of their properties. Having this as a precedent, Multiwalled carbon nanotubes are considered as a novel nanocarbon material, have been drawing increasing attention recently [65].

This type of carbon nanotubes (CNTs) is close to hollow graphite fibers, except that they have a much higher degree of structural perfection. Their graphite-like structure tube-wall, the nanometer-sized channel, the sp^2 carbon-constructed surface, and the excel lent performance of hydrogen adsorption and electron transport, make them promising in such applications as storage of hydrogen and some other gases, polymer additives and catalyst support material, adsorption–sepa ration medium, efficient field emitters, and electronic components (high-power electrochemical capacitors, high surface-area electrodes, etc.) [66].

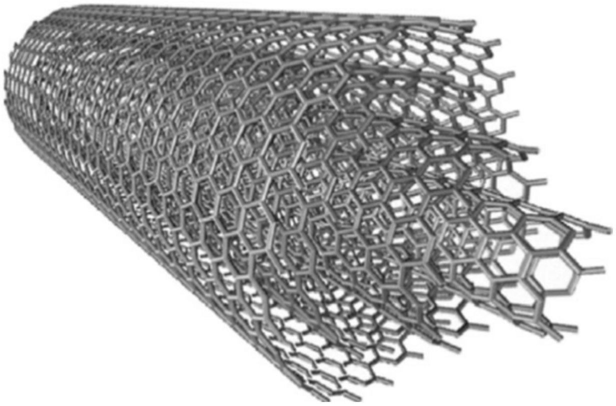

Fig 8 Representation of MWCNTs.

1.4 MWCNTs/Inconel 718 Nanocomposite

If the adhesion of the MWCNTs is linked to an increase in properties, it is highly desirable to go beyond what is already done and these are the nanocomposites which are high performance materials that exhibit combinations of unusual properties and unique design possibilities. They are formed by the union of two or more materials, in order to achieve the combination of mechanical and conductive properties. The properties of nanocomposites do not depend only on individual patterns, but also on their morphology.
Nanocomposites are high performance materials that exhibit combinations of unusual properties and unique design possibilities. With an estimated annual growth rate of 25%, its potential is so prominent that they are applicable in many areas [67].

Metal nanocomposite can also be known as reinforced compounds. Some of their functions are the protect the fibers or particles from the outside environment, the promote the union of the elements that constitute the reinforcement and give good resistance to corrosion or oxidation [68].

There are not many studies made about to develop Inconel 718 matrix compounds reinforced with carbon nanotubes. But there are different with metals matrix, resulting good thermal and electrical conductivity, high tensile strength to weight ratio, ductility and hardness [69], [70]. Many methods have been developed to manufacture MWCNTs-Metal compounds, such as cumulative rolling bonding, high energy ball mill [71], friction stir processing and powder metallurgy on scales [72].

Nanocomposites of MWCNTs in Inconel has been carried out through different processes such as adhesion of MWCNT arrays synthesized directly on nickel superalloy substrates employing a vapor-phase catalyst delivery method in a CVD chamber. [73] In this case, the carbon nanotube growth was carried out via floating catalyst thermal chemical vapor deposition using xylene as the main carbon source and ferrocene as a catalyst.

Another method of adhesion of MWCNTs is through Selective laser melting (SLM). Which is used for additive manufacturing. The MWCNT are coated with Inconel powder by mixing at the molecular level. Compared to the unprocessed Inconel sample, the results show a significant improvement in tensile strength and the final limit with less elongation. Also, with respect to the heat treatment in the composite sample it recovers its elongation to the level of pure Inconel while maintaining its maximum tensile strength but reducing its elastic limit [74].

The nanocomposites that are based on the adhesion of MWCNTs in matrices such as that of Inconel 718 also show innovation not only in their basic structure, but also thought that once created, it can have an improvement in the industry. An example of this is the adhesion of MWCNTs as nanofluids, which has been shown that once added the machinability is improved when processed, this leads us to consider that the adhesion of MWCNTs is not only intended for the basic process, but for an industrialized process [75].

1.4.3 CNTs oxidation

The adhesion of the CNTs to metal matrices is carried out through different processes where the dispersion of the CNTs is not taken into account. But if it were possible to distribute CNTs homogeneously in the matrix of any metal or alloy, it would be through a chemical interaction between the CNTs and the matrix. That is why this is thought of an oxidation of the surface walls of the CNTs that could lead to a good interaction if the matrix to which it will be added, also has affinity with the CNTs. This reactivity of organic compounds can be attributed to atoms or group of specific atoms within the molecule. A site of reactivity in an organic molecule is known as a functional group because it controls the behavior of the molecule. Thus, the chemistry of an organic molecule is largely determined by the functional groups it contains [76]. Chemical modification in carbon nanostructures is an area of study in materials science.
The most common methods used to carry out the functionalization are:

- Covalent Functionalization
- Non-Covalent Functionalization

2.1.4.1 Covalent Functionalization of CNTs

The process of covalent functionalization in carbon nanotubes has been studied from the point of view of carbon-carbon double-bond (alkene) reactions. The oxidation of alkenes can carry out the formation of functional groups by different types of reactions [77].

<u>Oxidation of alkenes</u>

Carboxylic acids can be obtained by breaking up alkenes with potassium permanganate in acidic or basic media and heating. This reaction generates products similar to ozonolysis, although instead of aldehydes it gives carboxylic acids (Figure 9).

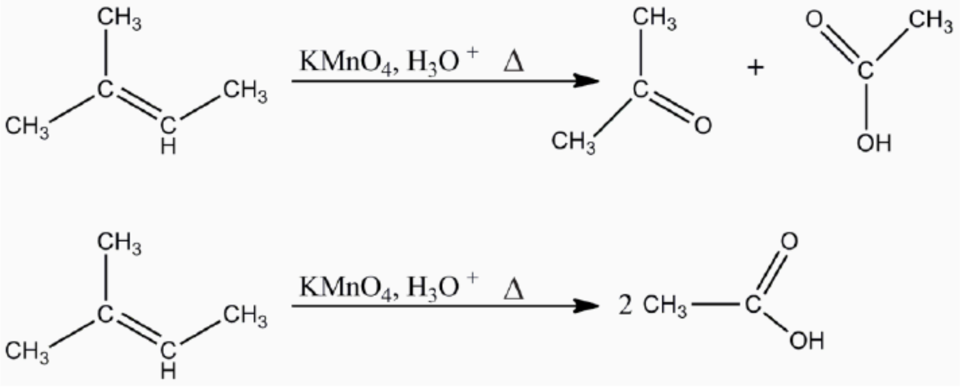

Fig 9 Oxidation of alkenes by potassium permanganate (KmnO4).

We can also obtain similar results from the oxidation of alkenes with ozone followed by treatment with hydrogen peroxide (Figure 10).

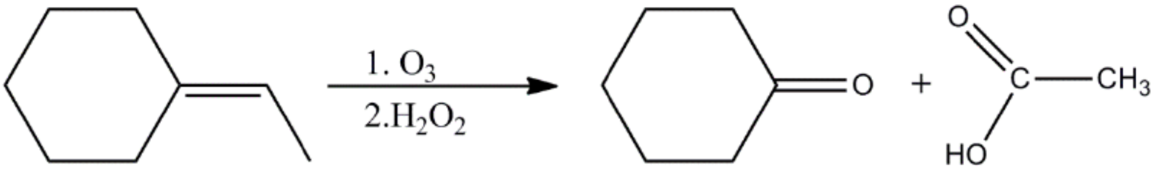

Fig 10 Oxidation of alkenes by ozone followed by hydrogen peroxide.

On the other hand, the hydration of alkenes is carried out with water. Water is a very weak acid, with insufficient proton concentration to initiate the electrophilic addition reaction. It is necessary to add an acid (H2SO4) to the medium for the reaction to take place. This reaction generates alcohols (Figure 11).

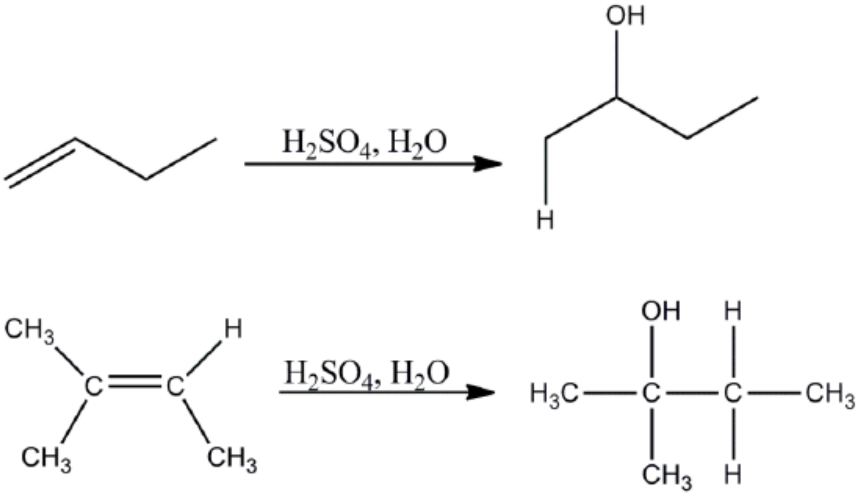

Fig 11 Oxidation of alkenes by hydration of alkenes.

Covalent functionalization in the walls is associated with a change in the hybridization of sp^2 to sp^3. The fluoridation of carbon nanotubes has been the subject of research for the onset of covalent functionalization because the side walls of the CNTs are inert [78], [79]. Fluorinated carbon nanotubes have weak C-F bonds (Figure 12) compared to alkyl fluorides [80] and provide substitution sites for further functionalization [81]. The replacement of fluorine atoms with amino, hydroxyl and alkyl groups has been shown.

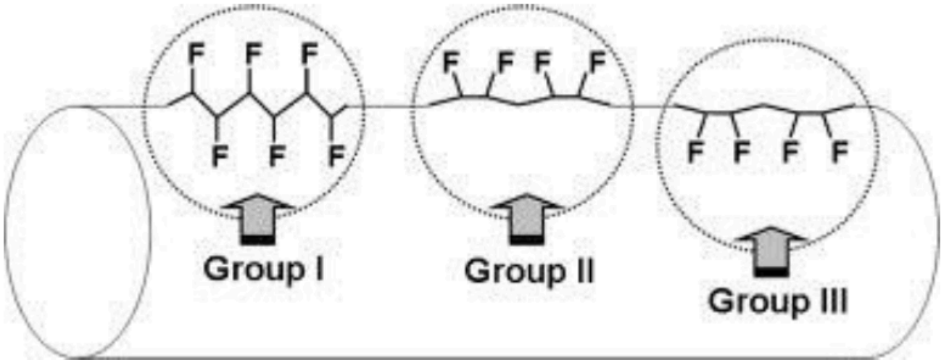

Fig 12 Formation of covalent bonds C-F.

Another method is the defects of carbon nanotubes. These defects are intrinsic and can be used to carry out oxidative damage to the structure of nanotubes by strong acids that leave holes functionalized with oxygenated functional groups [82]. In particular, treatment of CNTs with strong acid such as nitric acid (HNO3), sulfuric acid (H2SO4) or a mixture of them [83] or with strong oxidants such as potassium permanganate (KmnO4) [84], ozone [85], plasma reagent [86] tend to open these tubes to subsequently generate oxygenated functional groups such as carboxylic acid, ketone, alcohol and ester groups, which serve to anchor many different types of chemicals to the ends and defect sites of these nanotubes (figure 13). The chemical reactivity presented by these functional groups in carbon nanotubes can be used as precursors for additional chemical reactions, such as silanation, esterification, thiolation [85].

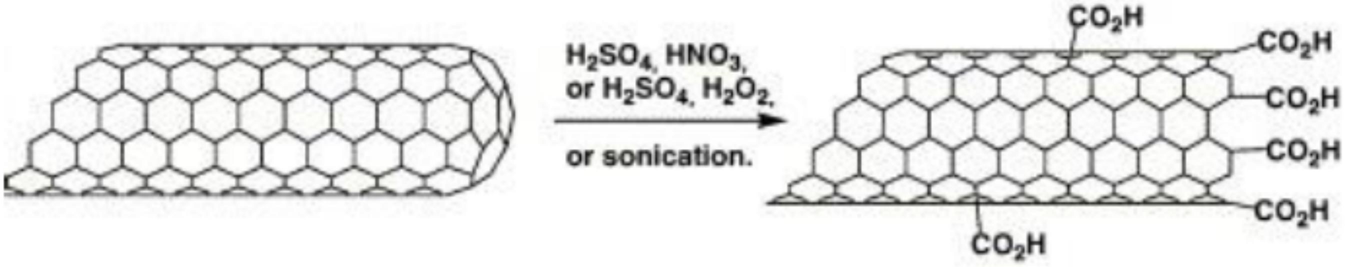

Fig 13 Scheme of chemical modification of carbon nanotubes by acid treatment for anchoring carboxyl groups – adapted from [86].

1.4.4 Metal-Matrix Functionalization

Considering the adhesion of the reinforcement phase, it is necessary to prepare the metallic phase, which will be processed by a functionalization in which carboxyl groups will be added on the surface, which will have a chemical affinity with the reinforcement phase, in this case, the MWCNTs. There are different ways to functionalize a metal matrix, however, the metal surface must be taken into account.

This is because from there it will be defined what will be the element that will give way to functionalization.

A very promising ally for the functionalization of Inconel 718 is citric acid which is a widely used surface-modifying ligand for growth and processing of a variety of nanoparticles; however, the inability to easily prepare derivatives of this molecule has restricted the development of versatile chemistries for nanoparticle surface functionalization. The synthesis of a derivative such as citric acid which has an alkyne group demonstrates that this molecule provides the ability to achieve stable, multi-carboxylate binding to metal oxide nanoparticles [87]. The broad utility of this strategy for the modular functionalization of metal oxide surfaces demonstrated its application in the modification.

Highlighting this assertion, the procedure proposed by S. Riaz which establishes that through a sol-gel process, the surface of Fe3O4 nanoparticles can be functionalized [88]. For making these nanoparticles useful in MRI contrast agent, nanoparticles were coated with citric acid. Citric acid (C6H8O7) is a short-chained molecule containing three carboxylate groups [89,90]. Citric acid gets adsorbed on the surface of superparamagnetic iron oxide nanoparticles (SPION) coordinating through one or two carboxylic group therefore leaving at least one carboxylic acid group unattached. This not only provides additional functionality but also prevents the agglomeration and oxidation of nanoparticles [91].

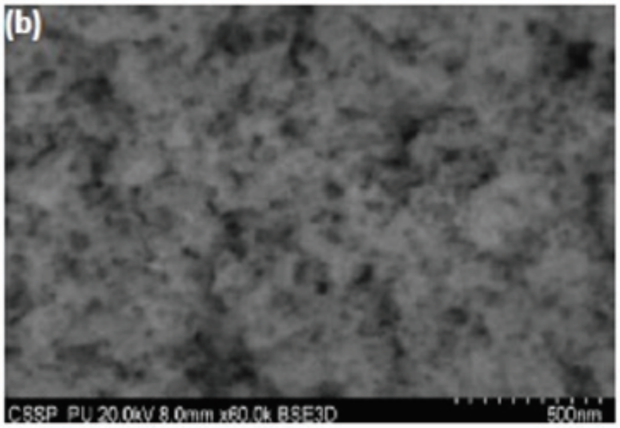

Fig 14 Fe3O4 coated with citric acid – Adapted from [88].

Citric acid also proves to be a good carboxylic acid capable of coating different oxidative surfaces such as ZnO, Fe2O3, TiO2, and WO3. This is stated by Lee M. Bishop, who uses citric acid on these metal oxides, making a kind of functionalization. This in order to leave the particles ready for later processes where the particle needs to have free carboxyl groups that serve as binders for some other adhesion [92]. The process of adhesion of citric acid to metal oxide is shown in figure 15.

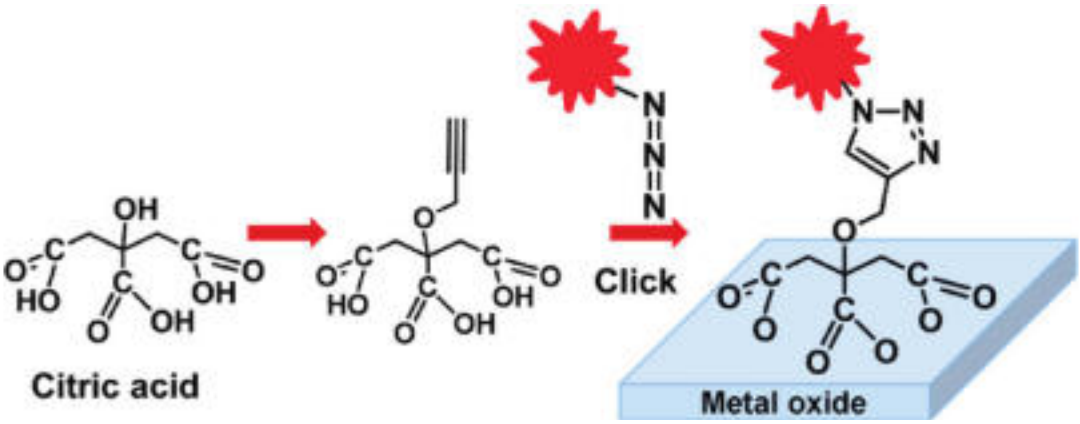

Fig 15 Representation of citric acid coating metal oxide surface, adapted from [92].

This leads us to think that citric acid can coat any metal particle by different routes increasing its surface reactivity. For example, Slavko Kralj states that it is feasible to make this functionalization of citric acid to iron oxide nanoparticles, which in their work were precipitated and used for the preparation of a stable aqueous suspension. Stipulating that a total of 5 ml of an aqueous solution of citric acid (0.5 g / ml) was added to the suspension of washed nanoparticles (approximately 2 g of particles in 60 ml of water) while stirring thoroughly. By doing this, two carboxylic groups of a citric acid dissociate, resulting in effective adsorption. This adsorption was promoted by heating the suspension at 80 ° C for 90 minutes. Due to this, the third carboxylic group of the adsorbed citric acid dissociates, increasing the surface charge of the nanoparticles, which provides electrostatic repulsions between the nanoparticles, preventing their agglomeration [93]. Which leads to establish that the citric acid particles manage to coat the metal oxide particles even when it is in very small concentrations.

The adhesion of carboxylic acids as a reactive surface layer asserts that if there is a reinforcer with this reactant affinity it is feasible to be able to have a chemical interaction which helps in a better adhesion and dispersion. A clear example would be the adhesion of MWCNTs to some metal matrix, as Lin Jiang puts it, which states that Al powder underwent surface modification to introduce a hydrophilic polyvinyl alcohol (PVA) membrane on its surface, which has good wettability and strong hydrogen bond interactivity with functionalized CNT. It was found that, when mixed with an aqueous suspension of CNT, PVA modified Al powder resulted in a much better CNT adsorption uniformity than untreated Al powder [45].

Following this assertion, a great similar example is established by Yu-Lin Hsin which states that Iron-filled multi-walled carbon nanotubes (Fe@MWCNTs) were surface functionalized with various functionalities via a rapid, single- step process involving ultrasonication assisted and microwave-induced radical polymerization reactions. Both hydrophobic (e.g., polystyrenes and polymethyl methacrylate) and hydrophilic (e.g., polyacrylamide, polyacrylic acids, and polyallyl alcohols) polymer chains can be chemically grafted onto the surface. The results showed good dispersion of MWCNTs when they were adhered to iron. [94]

1.4.5 Adhesion and dispersion of CNTs in a Metal-matrix.

When the functionalization processes for the metal matrix, such as the reinforcing phase is raised, it is necessary to think about a correct adhesion and dispersion of the reinforcing phase. A good approach to carry out this process is that established by Jian et al which gets "big concentrations" by doing what he calls the "suspension mix – suspension-based process". Jiang modified the surface of the aluminum powders using PVA thus increasing its wettability and improving its hydrophilicity. Jiang also used multi-wall hydrocarbon carbon nanotubes functionalized with carboxyl groups (-COOH), the preparation of CNT / Al compound powders is shown in Figure 15 suspension based on the mixing-suspension process [45]

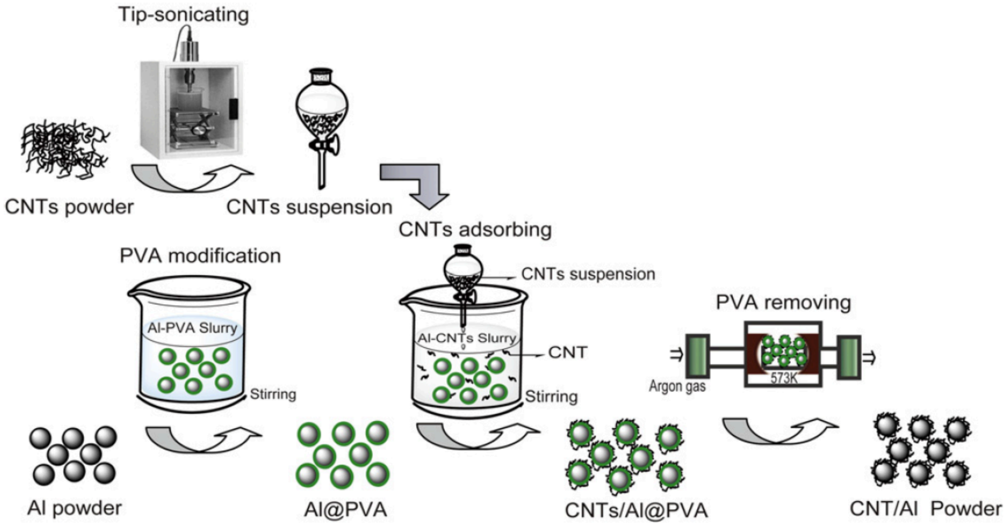

Fig 16 Fabrication procedures for CNTs/Al composite powder – Adapted from [45].

The wettability of Al powders was significantly increased by treatment with PVA and its hydrophilic nature, making the surface of Al powder compatible with that of functionalized CNTs, thus increasing the possibility of adsorption of CNTs to Al powder during the mixing stage We can see in Figure 16 (b) and Figure 16 (c) and that uniform adsorption of CNT is achieved by Al-PVA powders [45].

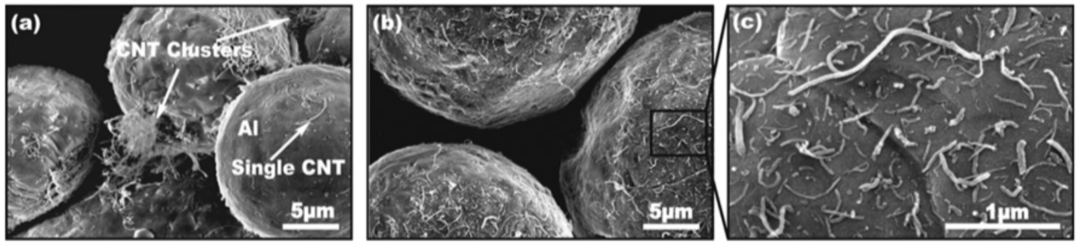

Fig 17 FE-SEM of CNT/Al powders. (a) CNT clusters in untreated Al powders, (b)-(c) uniform adsorption of CNTs achieved by Al-PVA powders. Adapted from [45].

In different circumstances, Seunggeun Jeon proposes to synthesize the GO capsulated on carbonyl iron particles (GOCIPs) by a simple wet stirring process. Also, the complex permittivity increases with the increment of the mass ratio of GO in GOCIPs from 0.5 to 2 wt % while the complex permeability values are not changed [95]. The process is described in the figure 15.

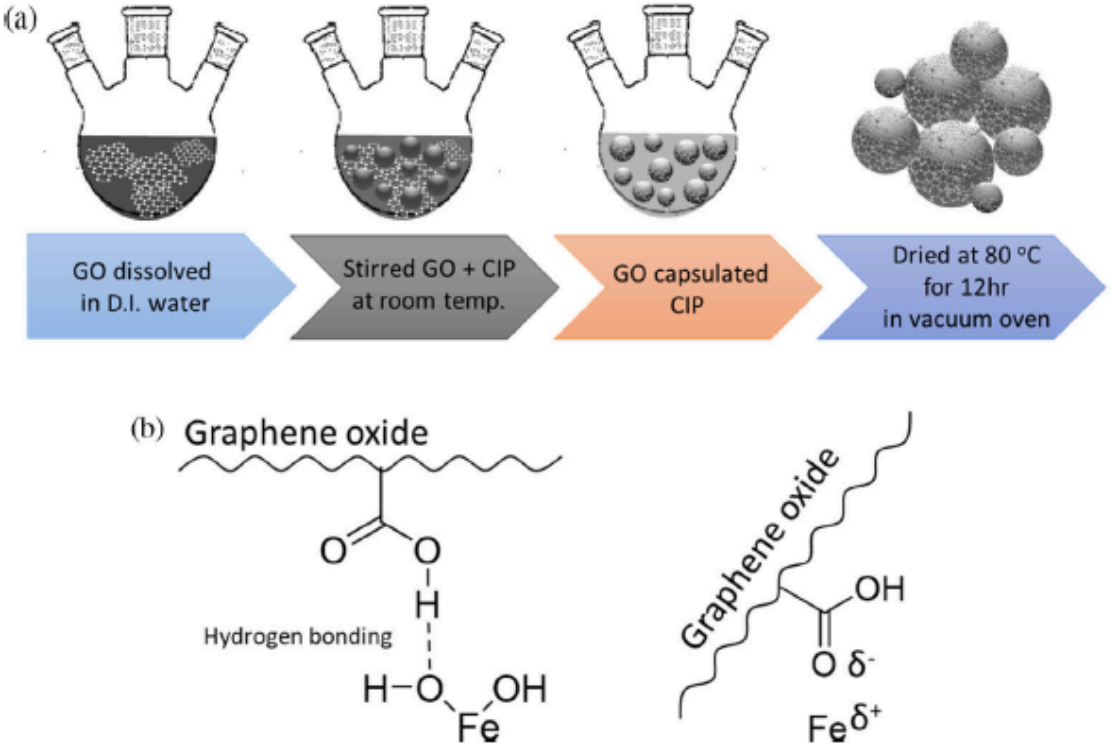

Fig 18 (a) A schematic of GOCIP synthesis process and (b) the possibility of GOCIP bonding mechanism – Adapted from [95].

1.4.6 Morphology and adsorption capacity in a Metal-Matrix nanocomposite

To create a change in the morphology in metallic powders, it is currently carried through the planetary ball mill, which due to collisions between balls and particles, changes in particle size and shape can be generated [96]. This can be a good option if it is said that giving a different morphology to the spherical in metals or superalloys such as Inconel 718, would lead to new ways of being processed and therefore, a range of different applications is considered.

Attempts like these have been made but in metals such as nickel, aluminum, iron itself, however, in order to create nanocomposites with better properties, it is proposed that superalloys can also go through similar processes [97]. A clear example is that posed by Xiangyu Zhao, who processed nickel powders with an average particle size of 30 mm and a purity of 99.9% through mechanical grinding. In this work the nickel powder was introduced into a stainless-steel container with stainless steel balls (10 and 6 mm in diameter) in an argon atmosphere. The ball-to-dust ratio was 20: 1. The grinding was done in a planetary mill with a rotation speed of 300 rpm and the grinding times were 5, 10, 20 and 40 h. And the result showed that after 40 h of grinding, the contamination by Fe, Cr and Mn of the grinding tools was less than 0.2% [98].

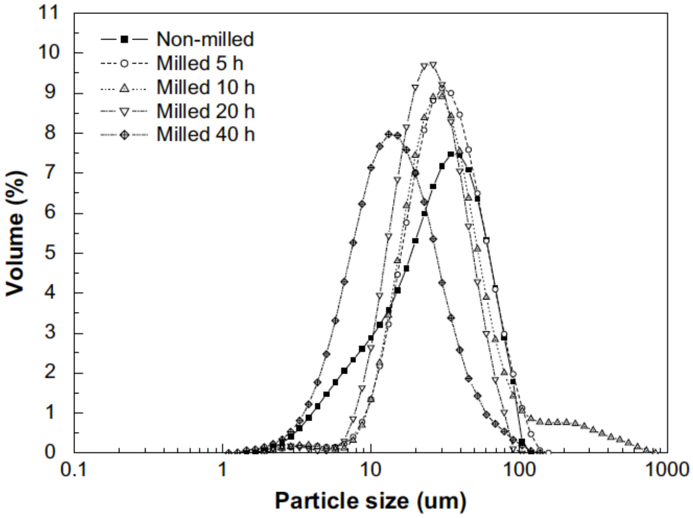

Fig 19 Particle size distributions of nickel powders for different milling times, adapted from [98].

Fig. 19 shows the distributions of the particle size of the nickel powders as a function of the milling time. The average particle sizes are 30.0, 33.9, 46.9, 26.2 and 18.2 mm for the milling time of 0, 5, 10, 20 and 40 h, respectively. It shows the change of the morphology of the powders milled several times. It can be seen that the morphology changes greatly after the mechanical milling. It is well known that cold welding and fracture are the two essential processes involved in the milling process.

If the particle size is related, with the percentage of adhesion of the reinforcing phase, better results are obtained when attaining adhesion. Since a flat morphology, contrary to a spherical, raises a surface more suitable for any adhesion in it. Taking this into account, once the desired morphology has been achieved, in this case a flake morphology, one can think about the correct adhesion and dispersion of the CNTs. These reinforced metal matrix composites have aroused much attention during recent years. This is resulted from their good mechanical and thermal properties. However, some problems related to the dispersion of CNTs in metal matrix can lead to difference between the expected and actual results. This initial step can be imagined as a more important level of Metal / CNT manufacturing procedure [99]. To overcome these problems, many of processing routes have been applied such as powder metallurgy, casting, melt infiltration, friction stir, thermal spraying and the other novel techniques.

The powder metallurgy-based methods have shown much research interest to achieve a uniform dispersion of CNTs within metal powder due to the lower temperature of process and better control of interface reactions between the matrix and reinforcement [100].

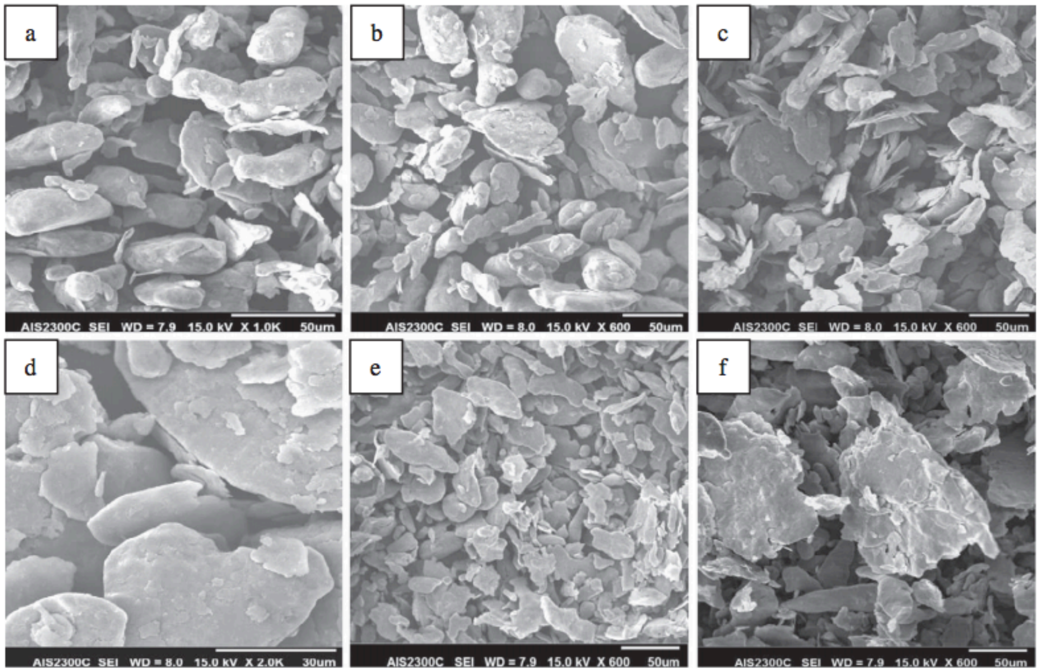

Fig 20 Evolution of morphology in aluminum matrix. Adapted from [100].

The subject of morphology modification and adhesion of CNTs is being investigated more strongly lately. Because this conjunction where a greater surface area of the material joins through the planetary ball mill and creates good adhesion of CNTs leads to a nanocomposite at a higher level. It gives way to more applications and an even larger field [101].

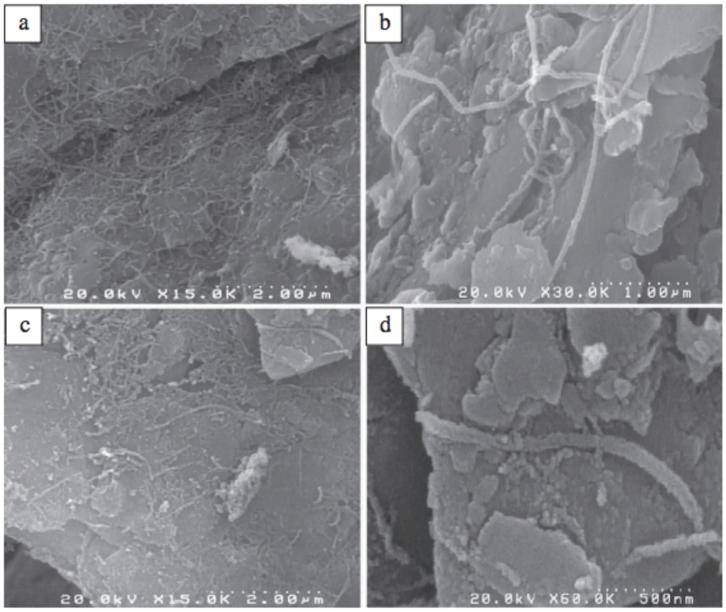

Fig 21 CNTs in aluminum matrix. Adapted from [100].

2 Chapter 2: Objectives and Hypothesis

2.1 General Objectives

To study the adhesion of CNTs on a superalloy surface developing a nanocomposite of Inconel 718 and Multi-Walled Carbon Nanotubes (MWCNT) for possible use in the aerospace field. This through 3 processes: the first step is the modification of the super alloy particle morphology due to the planetary ball mill. The second step is the functionalization of Inconel 718 and multi-wall carbon nanotubes (MWCNTS). And as a final step the adhesion and mixing of the two components.

2.2 Specific Objectives

- To generate a change in the morphology of Inconel 718 through the planetary ball milling.
- To functionalize Inconel 718 with carboxylic acid (citric acid) to induce carboxylic groups on its surface.
- To functionalize Multi-Wall Carbon Nanotubes through acidic means to induce hydroxyl groups mostly on its surface.
- To achieve a chemical interaction that generates better adhesion and distribution of the MWCNTs on the surface of the Inconel 718.
- To make the characterization and validation through instruments such as FT-IR, SEM, XRD, TGA.

2.3 Hypothesis

Inconel 718 will be modified in its morphology through the planetary ball mill to create two morphologies: Semi-spherical and flake. Each morphology will be functionalized with citric acid which will allow the induction of carboxylic acids on its surface. Similarly, the reinforcing phase, in this case, the MWCNTs, will be functionalized through acidic media resulting in oxidation on its surface allowing the induction of carbonyl groups. Due to the functional groups induced on the Inconel 718 and on the MWCNTs, there will be a chemical interaction between them that will give way to better adhesion and distribution of the MWCNTs on the Inconel 718.

3 Chapter 3: Experimental Methodology and Results

For the development of the nanocomposite created, different materials were used which were characterized by different techniques to have a solid base from where to start and where it would be reached. The main element, which was purchased by the Praxair company, is the Inconel 718. This is the super alloy that is taken as the metal matrix to study. The second important element to join are the MWCNTs, these were supplied by Sigma Aldrich. The MWCNTs play an important role in the matrix, since these were adhered so that once the nanocomposite can be consolidated, it adds better properties. On the other hand, there is citric acid which was supplied by Sigma Aldrich, and this is the bridge that will cause an interaction of the metal matrix towards the MWCNTs. Some other elements such as acids for the functionalization of MWCNTs were used, as well as products that made experimentation possible. These elements are listed in the following table.

3.1 Materials

Material	Supplier	Structure
Inconel 718	Praxair	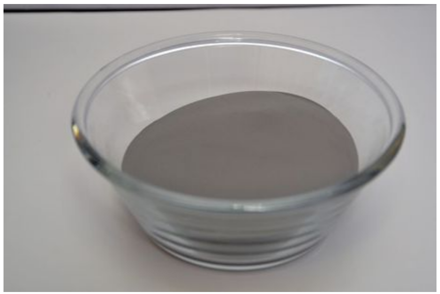 *Fig 22 Inconel 718 Powder.*
MWCNTs	Sigma Aldrich	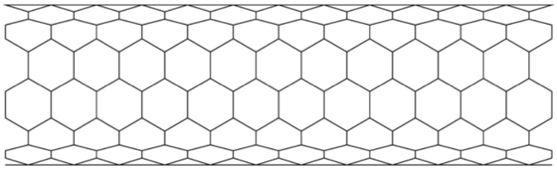 *Fig 23 MWCNTs structure.*

Citric acid	Sigma Aldrich	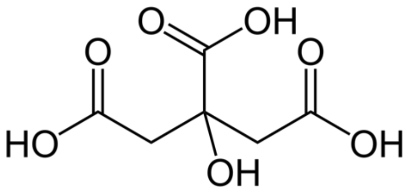 Fig 24 Citric Acid ($C_6H_8O_7$).
Parafilm	Sigma Aldrich	 Fig 25 Parafilm.
Acids	Sigma Aldrich	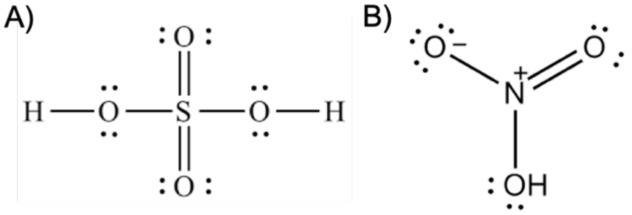 Fig 26 Acids used A) Sulfuric Acid (H2SO4), B) Nitric Acid (HNO3)

3.1.1 Main Rough Materials, characterization

The characterization of the base materials that were taken into account for experimentation was carried out by means of instrumentation such as SEM, EDS, XRD, FTIR and TGA. These characterization instruments yield results from chemical composition, surface images, grain size and boundaries, existing functional groups and degradations due to temperature. All these together make a thorough and comprehensive study of the materials used.

Inconel 718

The first element to analyze is the Inconel 718, which through SEM it was possible to verify that the dust as it was received came with an inhomogeneous particle size.

It is also appreciable that the morphology of the particles varies from elongated to spheres (fig. 27). This holds that for the modification of the same, it would have to be homogenized since otherwise, there would be no control.

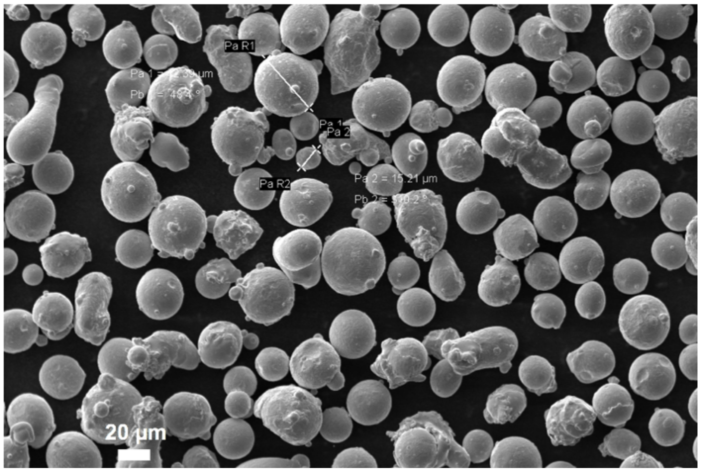

Fig 27 Characterization by SEM of Inconel 718 powder as received.

Subsequently, the characterization by means of EDS was taken to know the chemical composition of Inconel 718, even though the product already maintains a composition, it is important to check the existing proportion of elements in alloys such as these. On some occasions these go through processes which modify the composition in percentage of elements, so due to this the verification was done through EDS.

The characterization showed that in a timely manner, the 3 major elements in the alloy (nickel, chrome, iron) remained at that rate (fig. 28), even if the density percentage was lower. Elements such as titanium, niobium and Molybdenum are also found within the alloy. These elements add specific advantages to the alloy, such as corrosion resistance, grain size, hardness, among others.

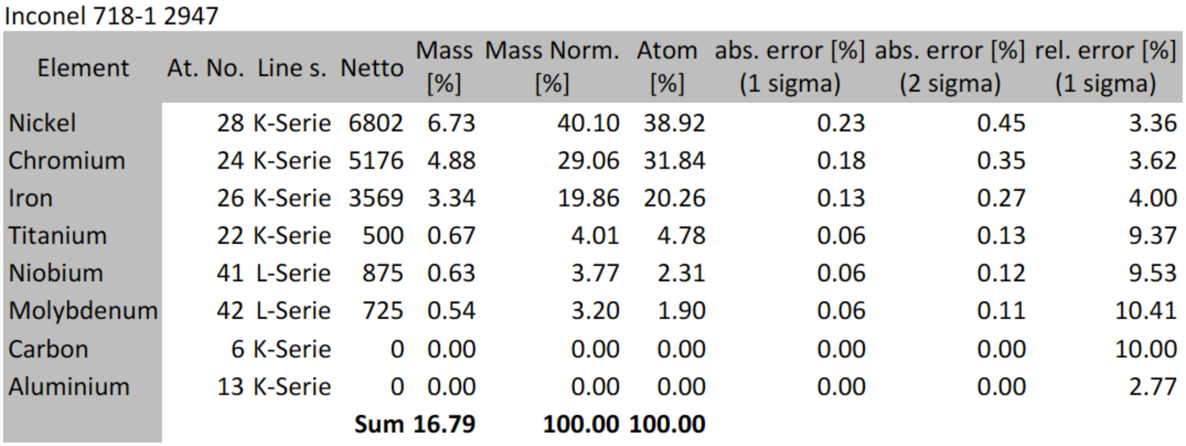

Inconel 718-1 2947

Element	At. No.	Line s.	Netto	Mass [%]	Mass Norm. [%]	Atom [%]	abs. error [%] (1 sigma)	abs. error [%] (2 sigma)	rel. error [%] (1 sigma)
Nickel	28	K-Serie	6802	6.73	40.10	38.92	0.23	0.45	3.36
Chromium	24	K-Serie	5176	4.88	29.06	31.84	0.18	0.35	3.62
Iron	26	K-Serie	3569	3.34	19.86	20.26	0.13	0.27	4.00
Titanium	22	K-Serie	500	0.67	4.01	4.78	0.06	0.13	9.37
Niobium	41	L-Serie	875	0.63	3.77	2.31	0.06	0.12	9.53
Molybdenum	42	L-Serie	725	0.54	3.20	1.90	0.06	0.11	10.41
Carbon	6	K-Serie	0	0.00	0.00	0.00	0.00	0.00	10.00
Aluminium	13	K-Serie	0	0.00	0.00	0.00	0.00	0.00	2.77
			Sum	**16.79**	**100.00**	**100.00**			

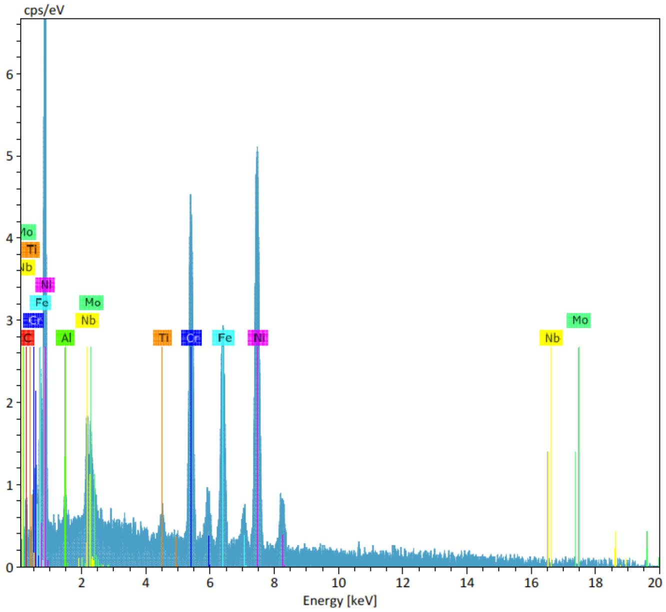

Fig 28 Characterization by EDS to know chemical composition of Inconel 718.

The XRD characterization of Inconel 718 reflects the diffraction planes derived from the alliating materials, in this case the three main ones. Mostly the existing planes are nickel (fig. 29), but it can also see iron and chrome planes around 45 and 50. These diffraction planes are well identified in literature, however not as an alloy, but as each of the characteristic elements.

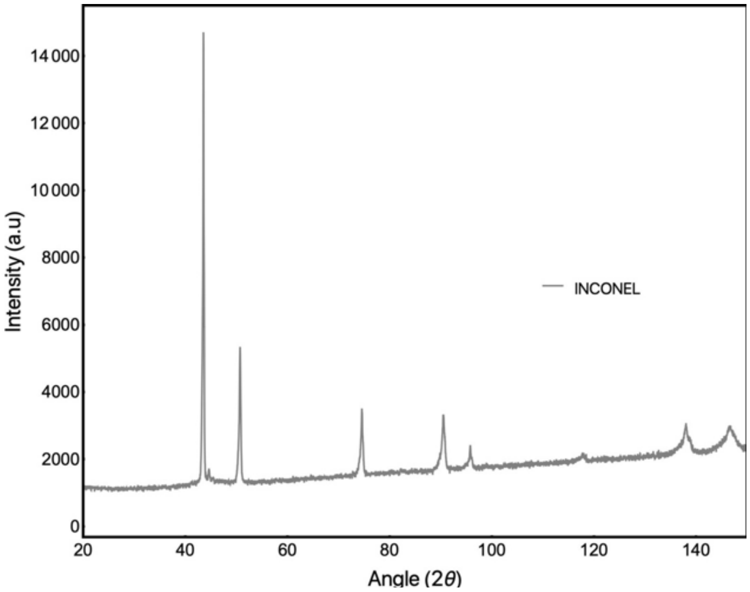

Fig 29 Characterization by XRD of Inconel 718 powder as received.

Because there was an adhesion of functional groups anchored to the metal matrix, Inconel 718 was characterized by FTIR. This characterization technique showed that there may be existing bands (fig. 30) even when the material is metal and should not have these bands present. However, this is possible since Inconel 718 goes through a series of previous processes to be able to form as an alloy, and these processes can induce oxides, or small chemical interactions that are disposable since they do not affect experimentation.

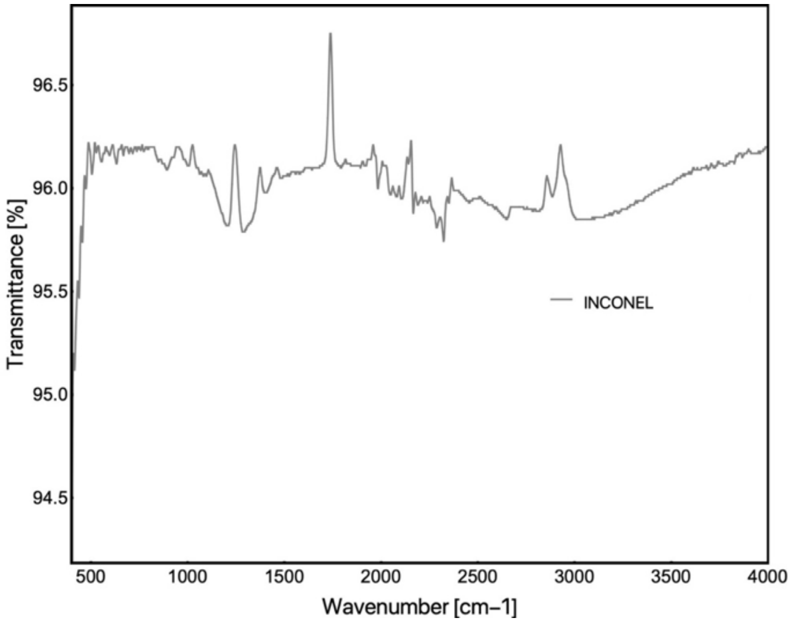

Fig 30 Characterization by FTIR of Inconel 718 as received.

Multi-Wall Carbon Nanotubes

In the case of the Multi-Wall Carbon Nanotubes, the first characterization was carried out by means of SEM, this in order to be able to identify them visually and once added to the metal matrix it would be more feasible to see them. If we enter the image of SEM, it is notable to appreciate that the MWCNTs in the way they were received are agglomerated in some areas (fig. 31), these decrease with the subsequent functionalization performed. However, it is important to emphasize that industrial grade MWCNTs such as those used in this case, maintain a low degree of purity and distribution.

It is possible that these carbon phases existing in industrial grade MWCNTs can be reflected in the subsequent characterizations, since they cannot be eliminated, but they can be reduced with a good distribution of MWCNTs in solution before being added to the metal matrix.

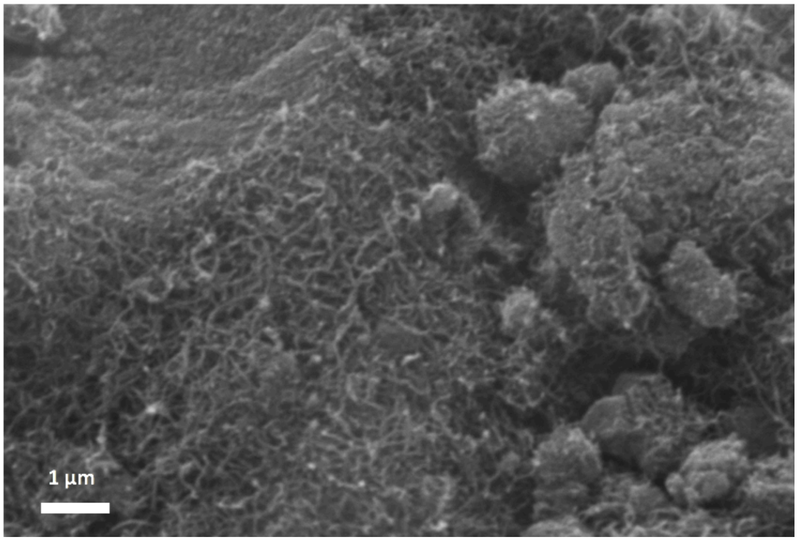

Fig 31 Characterization by SEM of MWCNTs as received.

The carbon phases that MWCNTs provide are reflected in the characterization by means of XRD, here the diffraction plane between 25-30 is noticeable (fig. 32). If a correct adhesion of the MWCNTs in the metallic matrix is achieved, it would be reflected in the same way, which is why it is so important to be able to characterize the MWCNTs alone.

Analyzing further the diffraction planes it is notorious to see replicas between 45-55, these only indicate different accommodations of the same existing carbon, however the one that stands out and has as a reference for its intensity in the plane, it is the first (between 25 -30).

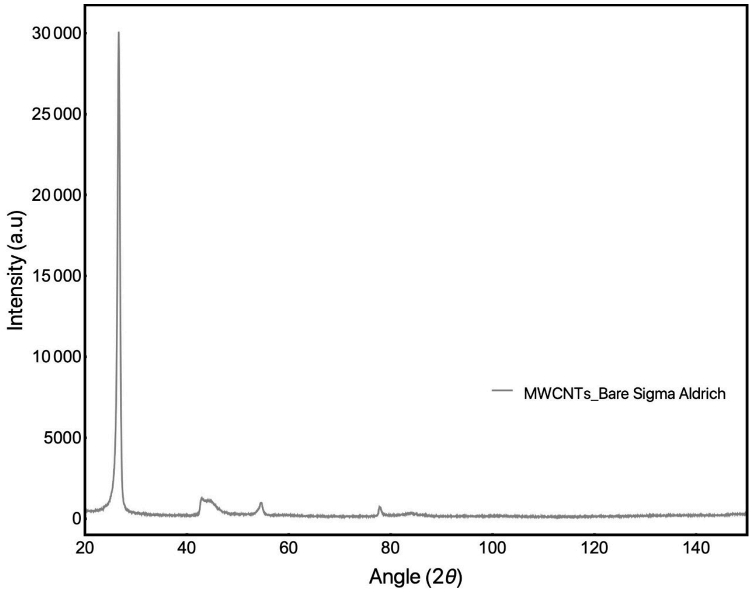

Fig 32 Characterization by XRD of MWCNTs as received.

The characterization by means of TGA of the MWCNTs (figure 33), showed that in an oxygen environment they are degraded at a temperature of 580 ° C. What gives guidance that once attached to the metal phase this will be a point of reference to know where to place them when doing a TGA analysis again with the nanocomposite already created.

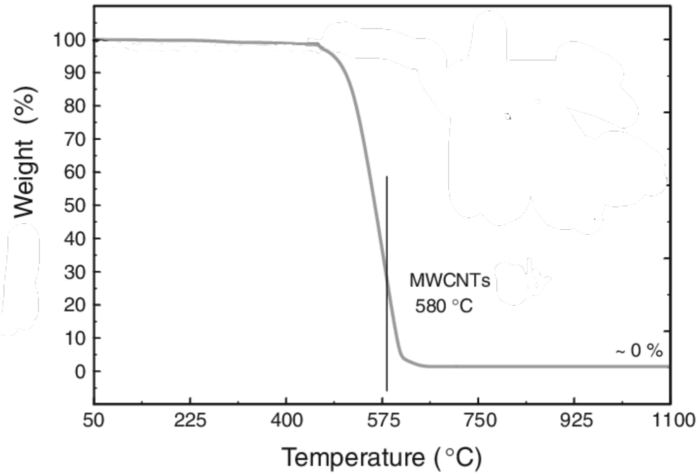

Fig 33 Characterization by TGA of MWCNTs as received.

Citric Acid

Analyzing the citric acid by means of TGA (fig. 34), it was possible to observe a drop-in weight around 200 ° C, it should be noted that the environment used was in oxygen. This indicates that a degradation of citric acid must be found in the vicinity when the nanocomposite is characterized.

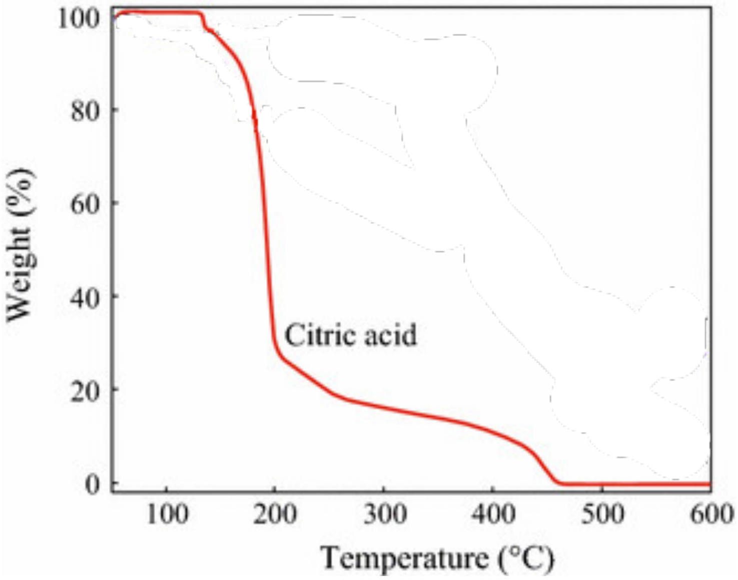

Fig 34 Characterization by TGA of Citric Acid as received.

The FTIR characterization of citric acid yielded existing bands between 1750, with a replica around 3250 (fig.35). This is due to the existing carboxy groups, which are double carbon-oxygen bonds and simple oxygen-hydrogen bonds.

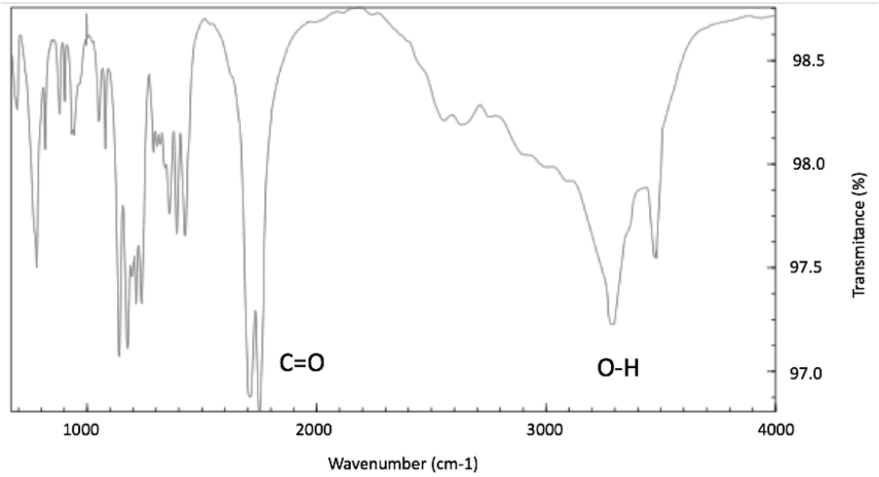

Fig 35 Characterization by FTIR of Citric Acid as received.

3.2 Processing experimental routes

For this work, different processing paths were designed as shown in the following diagram:

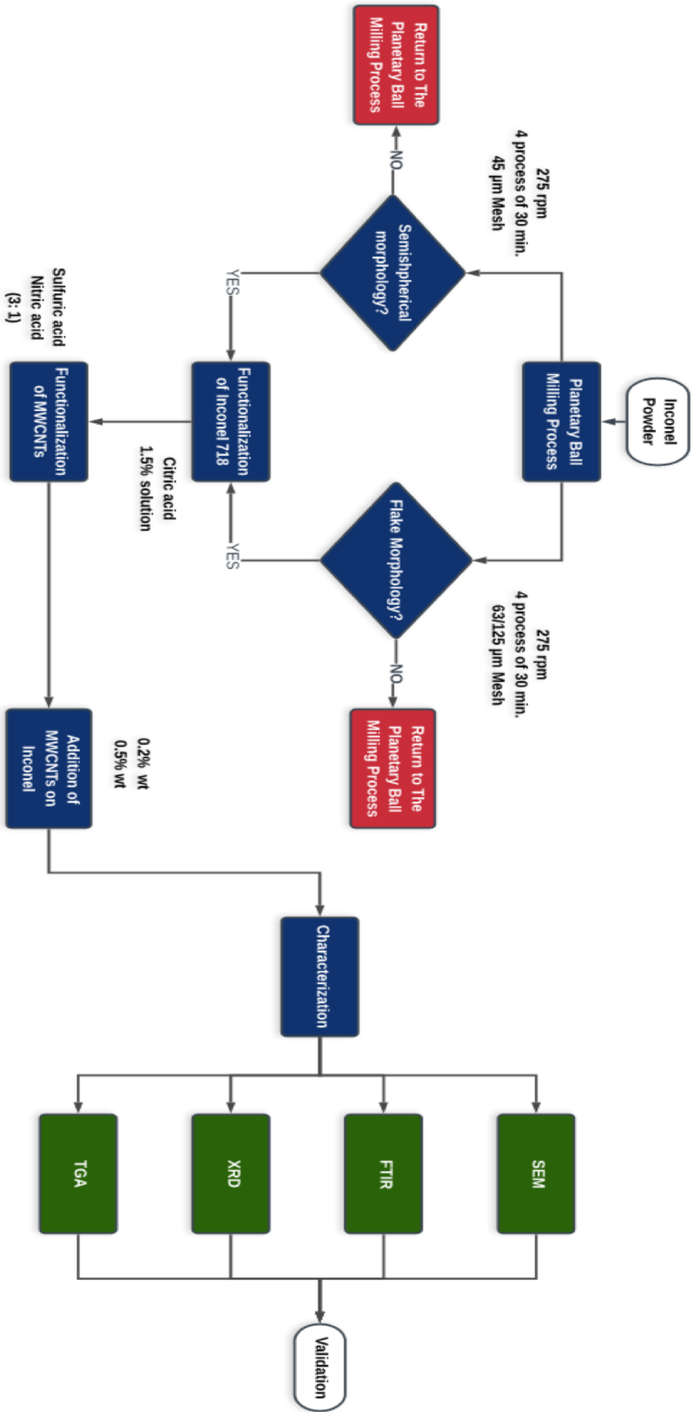

Fig 36 Diagram of the different process routes.

The work done in the planetary Ball Milling is described in table 6:

Methodology / Technique	Experimental Stage	Processing route	General objective	Parameters
				Two milling process
Planetary Ball milling	Stage 1	Test A	Change the morphology	220 rpm 30min
Planetary Ball milling	Stage 2	Test A	Change the morphology	250 rpm 30min
Planetary Ball milling	Stage 3	Test A	Change the morphology	275 rpm 30 min
Planetary Ball milling	Stage 4	Test A	Change the morphology	300 rpm 30 min
Planetary Ball milling	Stage 5	Test A	Change the morphology	325 rpm 30 min
Planetary Ball milling	Stage 6	Test A	Change the morphology	350 rpm 30 min
Planetary Ball milling	Stage 7	Test B	Control of the morphology	275 rpm 90 min
Planetary Ball milling	Stage 8	Test B	Control of the morphology	275 rpm 30 min
Planetary Ball milling	Stage 9	Test C	Control of the morphology	275 rpm 30 min
Planetary Ball milling	Stage 10	Test C	Control of the morphology	275 rpm 30 min
Planetary Ball milling	Stage 11	Test C	Control of the morphology	275 rpm 30 min
Planetary Ball milling	Stage 12	Test C	Control of the morphology	275 rpm 30 min

Table 6 Experimental design and processing routes.

3.3 Ball-Milling process

3.3.1 Procedure

The planetary ball milling process entails a series of steps that are listed below:

1. Weighing of materials.
2. Mixing of the materials and the balls (inert atmosphere).
3. Milling process.
4. Powder sieving.

<u>Weighing of materials</u>

- Weigh 100 grams of Inconel 718 in a closed container, which has a volume meter as It is around 40 ml.
- Weigh 200 grams of balls in a closed container, which has a volume meter since for balls of 2 millimeters in diameter It is around 40 ml.

Fig 37 Weighted Inconel 718 and balls in closed containers.

Mixing of the Inconel 718 and the balls (inert atmosphere)

- Connect the AtmosBag to an inert gas line and to a vacuum pump. (For this step we used argon gas.)
- Introduce the milling Jar, the closed containers with the balls, Inconel 718 and 2.5 squares long piece of parafilm.
- Seal the AtmosBag.
- Turn on the vacuum pump to get oxygen out of the AtmosBag.
- Fill the AtmosBag with an inert gas.
- Repeat the last two steps three times.
- With the inert atmosphere inside the AtmosBag mix the Inconel 718 and the balls into the milling Jar.
- Seal the system with the Milling Jar lid and the 2.5 squares of parafilm.
- Take the jar out of the AtmosBag.

Fig 38 Sealed Jar with Inconel 718 and the balls inside.

Milling process

- Place the jar in the mill.
- Fix the container
- Set the time and the speed of the process
- At the end of the process, be careful not to open immediately the container, the milling process could increase the temperature of the material, and in the presence of oxygen some powders could explode.

Fig 39 Fixed Jar in the mill.

Powder sieving

- Place the different sieves in the sieve shaker.
- Empty the Jar into the sieves.
- Fix the sieves to the equipment.
- Set the amplitude and time for the process.
- For this work we used an amplitude of 40 and a time of 10 minutes.
- Weigh the material in the collecting pan.

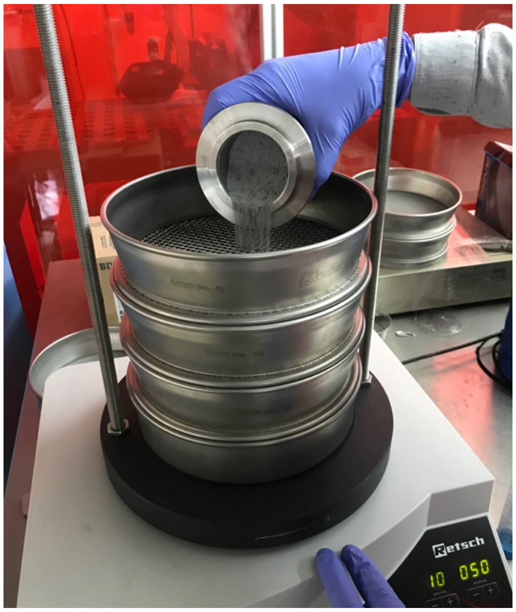

Fig 40 Moment just before the sieving process.

3.3.2 Equipment

3.3.2.1 *Planetary Ball Mill*

Fig 41 Planetary ball mill.

The planetary ball mills can be used for all those applications in which very fine granulometries must be obtained. In addition to the classic crushing and mixing processes, these mills comply technically with all the requirements for colloidal grinding and have the necessary energy efficiency to make mechanical alloys. The extremely high centrifugal force of these planetary ball mills generates a very high crushing energy, which translates into very short grinding times.

For these experiments we use the Retsch brand PM 100 which is a compact benchtop unit with a grinding station.

3.3.2.2 *Vibratory Sieve Shaker and Sieves*

Fig 42 Vibratory sieve shaker and sieves.

The analytical sieves are used in the areas of research and development, quality control of raw materials, intermediate products and finishes, as well as in the supervision of production processes. The regulated electromagnetic drive allows an optimal adaptation to any type of material. These machines convince by their great separation precision in short sieving times.

We use the AS 200 basic of the RETSCH brand. Which has adjustment and digital display of the performance and sieving time.

3.3.2.4 AtmosBag

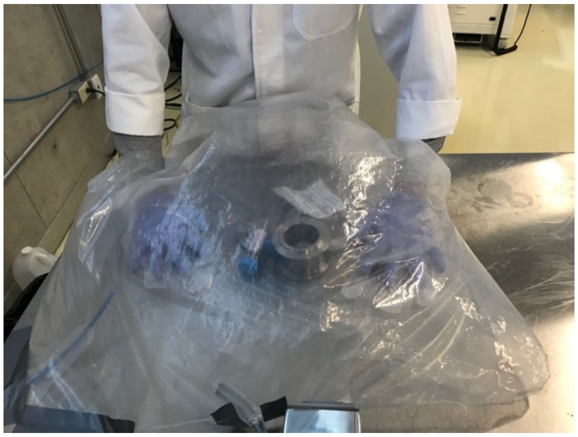

Fig 43 Atmos bag glove Bag with zipper-lock closure by Sigma-Aldrich.

Atmos Bag glove bag is a flexible, inflatable polyethylene chamber with built-in gloves that lets you work in a totally isolated and controlled environment. It is an inexpensive, portable alternative to the glove box and is well suited to a variety of tasks and materials.

3.4 Inconel 718 + MWCNTs: Chemical functionalization process

3.4.1 Procedure

The adhesion process has proved to be a good technique to achieve good dispersion of the MWCNTs. It was used to disperse them on the particles of Inconel 718 and thus achieve greater effectiveness of the desired objective.

This process entails a series of steps that are listed below:

1. MWCNTs functionalization.
2. Inconel 718 powder functionalization.

3. Adsorption of the functionalized MWCNTs on the Inconel 718 functionalized powder.

MWCNTs Functionalization

- Through a chemical oxidation process
- Prepare an acid solution using HNO_3 and H_2SO_4 in 1:3 proportion.
- Suspend 100 mg of MWCNTs in 20 ml of the acid solution prepared before.
- Sonicate for 24 h.
- Dilute the suspension with 500 ml of deionized water.
- Collect the MWCNTs with 100-nm pore membranes.
- Filter the MWCNTs.
- Wash until obtaining a neutral PH.

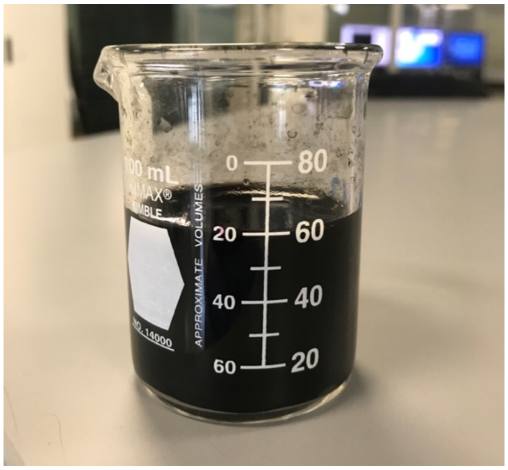

Fig 44 Functionalized MWCNTs.

Inconel 718 powder functionalization.

- Weigh 2.5 grams Inconel 718 powder.
  0.66% solution-wt. citric acid (200 milligrams).
  12.5 miligrams of MWCNTs.
- Inconel citric acid Aqueous solution.
  - Disperse the 200 milligrams of citric acid powder in 30 ml deionized water.
  - Constant stirring for 1h.
  - Raise the temperature to 90ºC
  - Disperse the 2.5 grams of Inconel 718 powder
  - Constant stirring for 1h.
  - Filter the powders.
- Filter
  - We used a Sterifil aseptic system with a vacuum pump.
  - One membrane was used.
- Dried up
  - Leave in the flask for 12 hours at a temperature of 120 ℃.

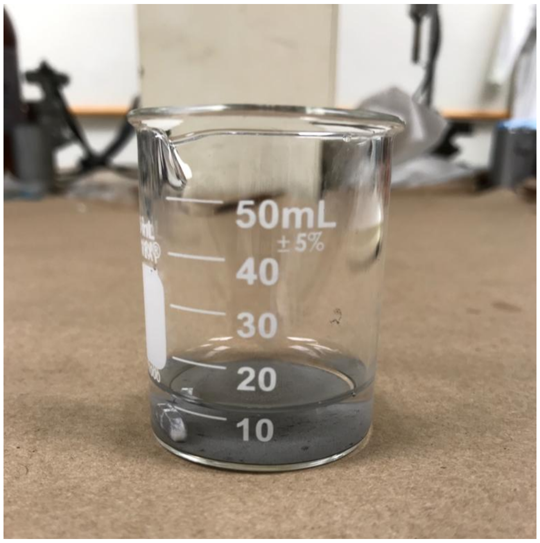

Fig 45 Functionalized Inconel 718.

Adsorption of the functionalized MWCNTs on the Inconel 718 functionalized powder.

- Weigh 2.5 grams Inconel 718 powder and put it in a solution with 20 ml of distilled water.
- Adhesion of MWCNTs.
  - Adhere the MWCNTs (1 mg / ml solution) by dripping to the Inconel 718 solution with distilled water.
  - Constant stirring.
  - We stop adding MWCNTs until it is impossible to see the phase difference.

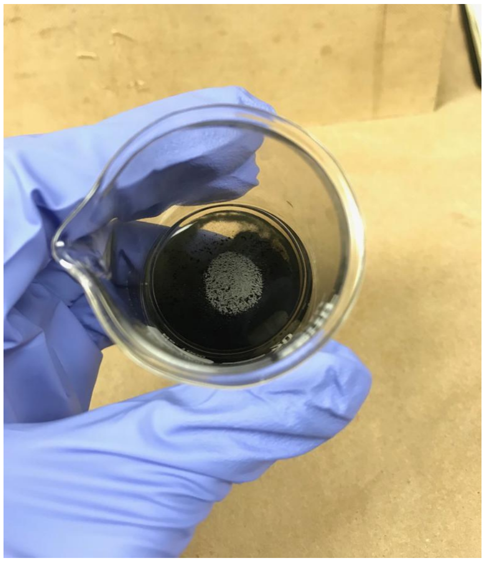

Fig 46 Phase differentiation between Inconel 718 and MWCNTs.

3.4.2 Equipment

3.4.2.1 Magnetic Stirrer and Hot Plate

Fig 47 Magnetic Stirrer and hot plate.

The Magnetic stirrer with hot plate is a device that, through the conduction of heat, allow us to raise the temperature of different objects, substances and/ or materials in a constant and uniform manner.

3.4.2.2 Ultrasonic Bath

Fig 48 Ultrasonic Bath.

The ultrasonic bath applies sound energy to agitate the particles of a sample. An electric current transmits its energy to a mechanical system that will convert it into high intensity vibrations. Within the liquid, millions of microscopic bubbles will be generated, these bubbles undergo rapid expansion and collapse processes that can transmit their energy to the materials in the bath.

3.5 Size statistic

The statistics made for the particle size distribution showed that for the semi-spherical particles it was possible to modify the diameter size between 30 and 40 µm. This measure being mostly, however it is notable to consider that smaller and larger particles still exist.

With the flake particles the change in morphology was more drastic, throwing a length size between 110 and 120 µmon. mostly. By determining that as appropriate in the industry, controlled particle sizes could be used as required by the application.

4.5.1 Semi-Spherical Morphology

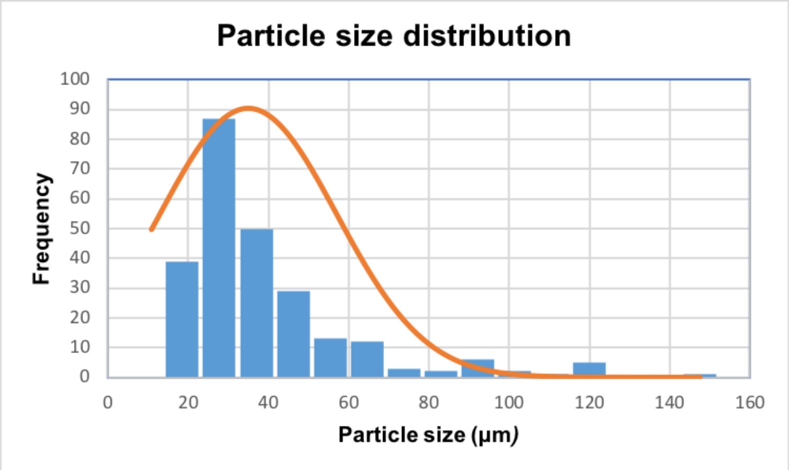

Fig 49 Particle size distribution of Semi-spherical morphology.

4.5.2 Flake Morphology

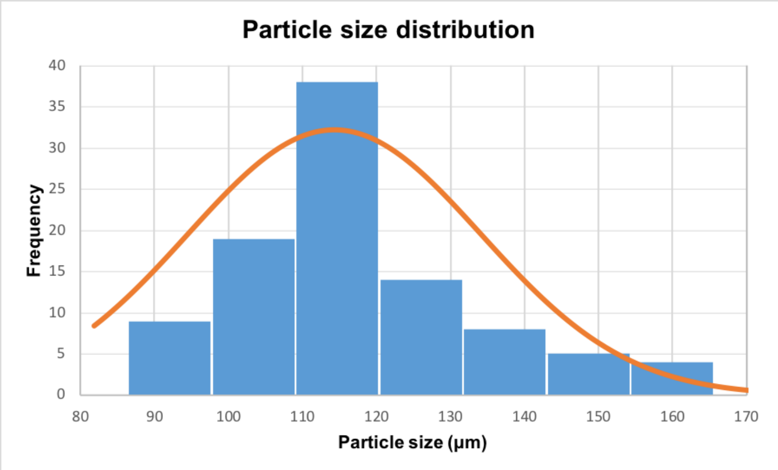

Fig 50 Particle size distribution of flake morphology

4 Chapter 4: Results and Discussions

4.1 Ball milling Process

4.1.1 Semi-Spherical Morphology

In the present work, Inconel 718 was characterized by means of SEM. Where two morphologies were reached, the first is hemispherical morphology, which complied with the hypothesis. Moving from a spherical to a hemispherical morphology as can be seen in figure 51. Having a particle size range of 30 µm to 50 µm.

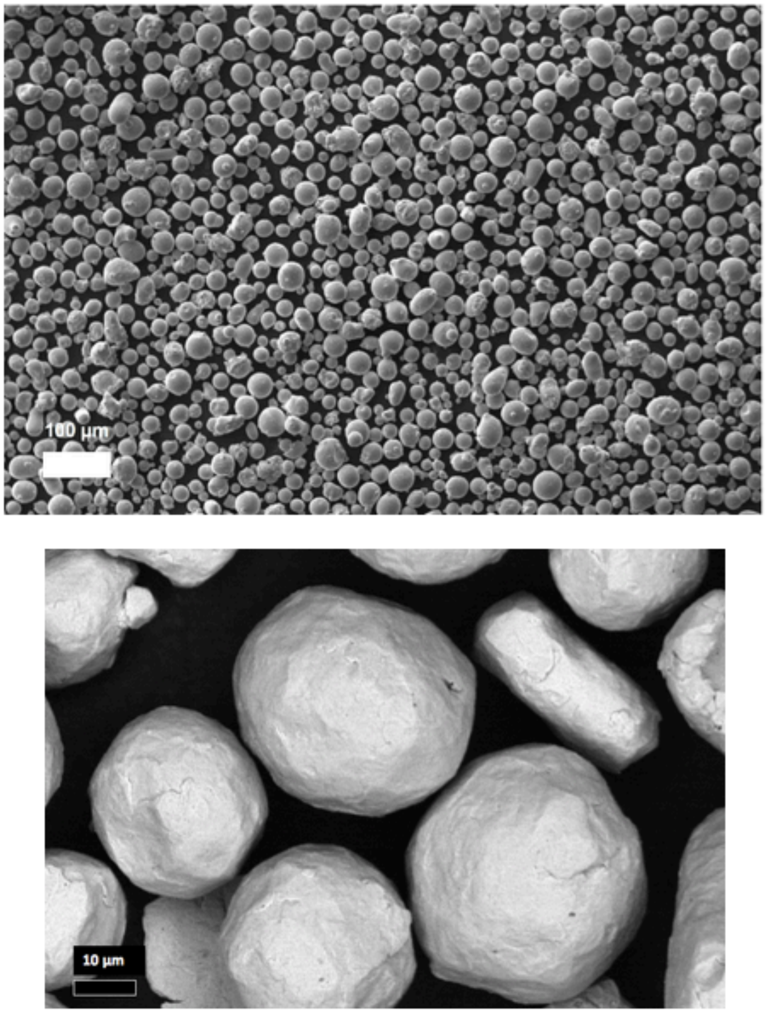

Fig 51 Semi-Spherical morphology by SEM.

4.1.2 Flake Morphology

In the case of flake morphology, we were able to develop particle sizes from 63 µm to 250 µm. This depends on the sieves we will use to sift the powder once it has been modified. This is consistent with the hypothesis where it was proposed that it was possible to modify the morphology to make this type of flake morphology. So, during the process we could find these three ways to develop them to obtain different sizes.

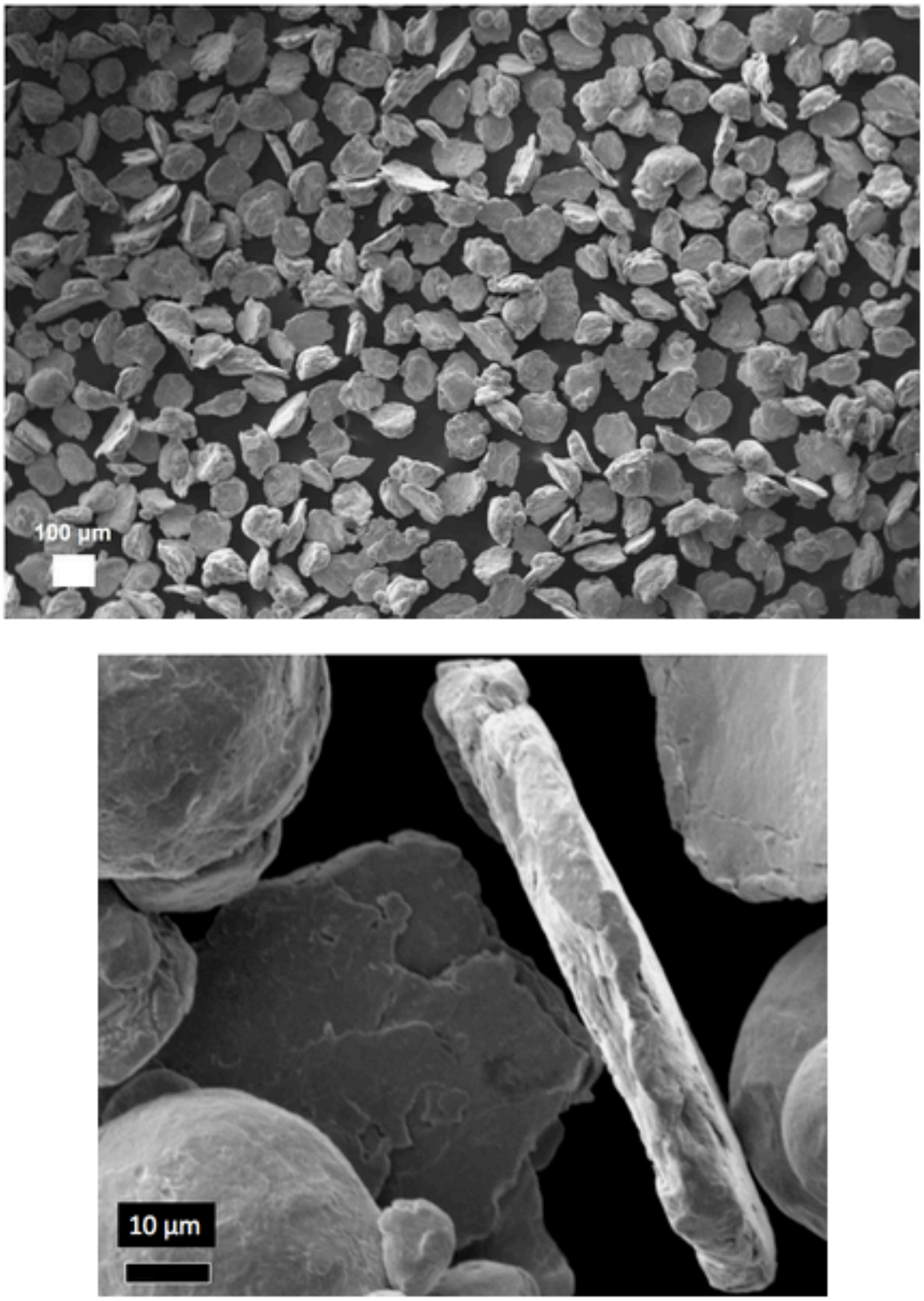

Fig 52 Flake morphology by SEM.

4.2 Functionalization of Inconel 718

4.2.1 Inconel 718 Semi-Spherical with Citric Acid

The functionalization of the Inconel particle with semi-spherical morphology was carried out and characterized by SEM. However, in SEM it is not possible to differentiate whether the particle is coated with citric acid, but it could be seen that the particles began to agglomerate once coated (Figure 53). This is a change that did not happen with the Inconel particles alone, so it can be a starting point that indicates the presence of something else, in this case citric acid.

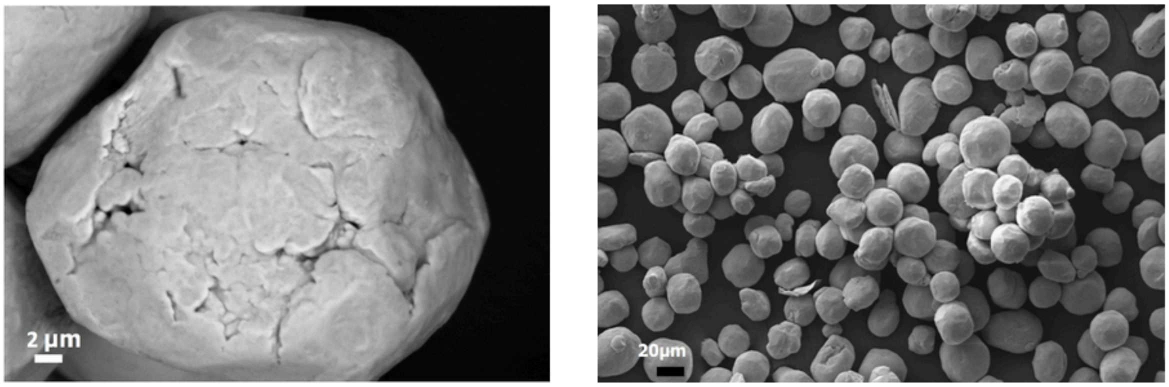

Fig 53 Semi-spherical morphology with citric acid by SEM.

The characterization of Inconel 718 with citric acid by means of XRD (fig. 54) does not show any change in any diffraction plane, only the characteristic planes of Inconel 718, because citric acid does not show planes within the spectrum.

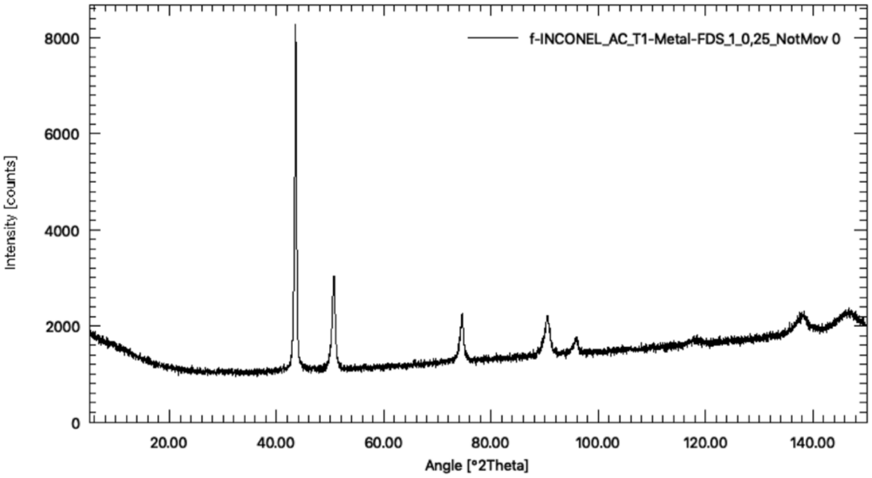

Fig 54 Semi-spherical morphology with citric acid by XRD.

The bands found for citric acid in Inconel 718 (fig. 55) were between 1600-1750, with a replica between 3200-3500, which indicate the presence of carbonyl groups that are characteristic of citric acid, denoting the presence in Inconel particles 718.

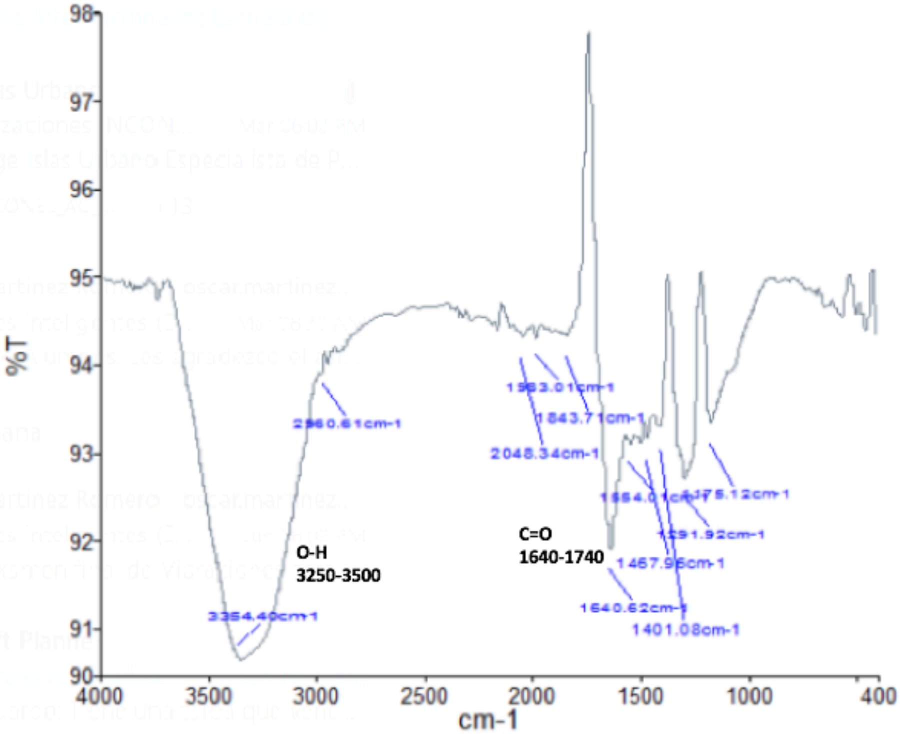

Fig 55 Semi-spherical morphology with citric acid by FTIR.

4.2.2 Inconel 718 Flake with Citric Acid

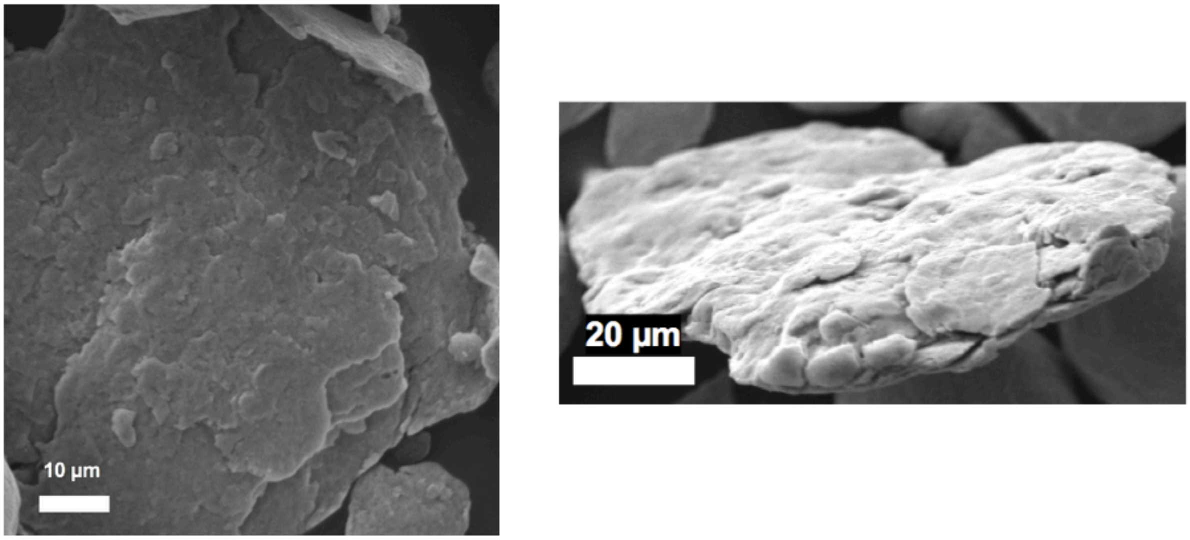

Fig 56 Flake morphology with citric acid by SEM.

The functionalization of the Inconel particle with flake morphology was characterized by SEM. However, in SEM it is not possible to differentiate whether the particle is coated with citric acid, but it can be seen that the adhesion of citric acid does not affect morphology. (Figure 56).

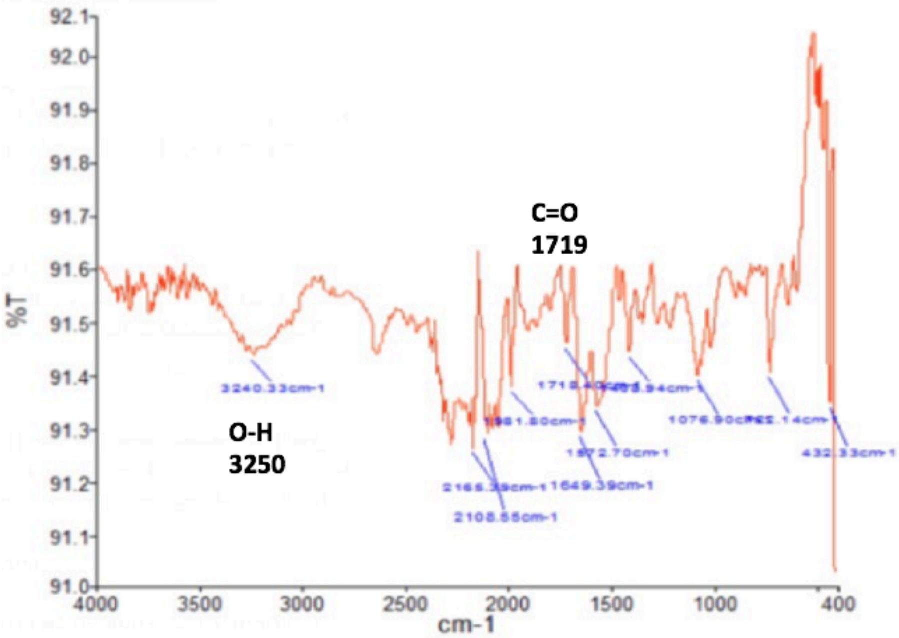

Fig 57 Flake morphology with citric acid by FTIR.

Like the semi-spherical particles, when functionalizing Inconel particles with flake morphology it was possible to see the bands between 1600-1750, with a replica between 3200-3500 (fig. 57), which indicates the presence of carbonyl groups that are characteristic of citric acid, which denotes the presence in Inconel particles 718 with flake morphology.

This indicates that no matter what morphology you have, once the functionalization process has been carried out by adding citric acid, it will be able to adhere to the Inconel 718 particle. So, it works for the two morphologies with which it was worked.

4.3 Functionalization of MWCNTs

The functionalization of the MWCNTs resulted in a better dispersion, having less agglomeration. This can be seen through the SEM images (fig. 58) which show an improvement. However, there are still agglomerates but these have decreased making the comparison between non-functionalized MWCNTs and those that are.

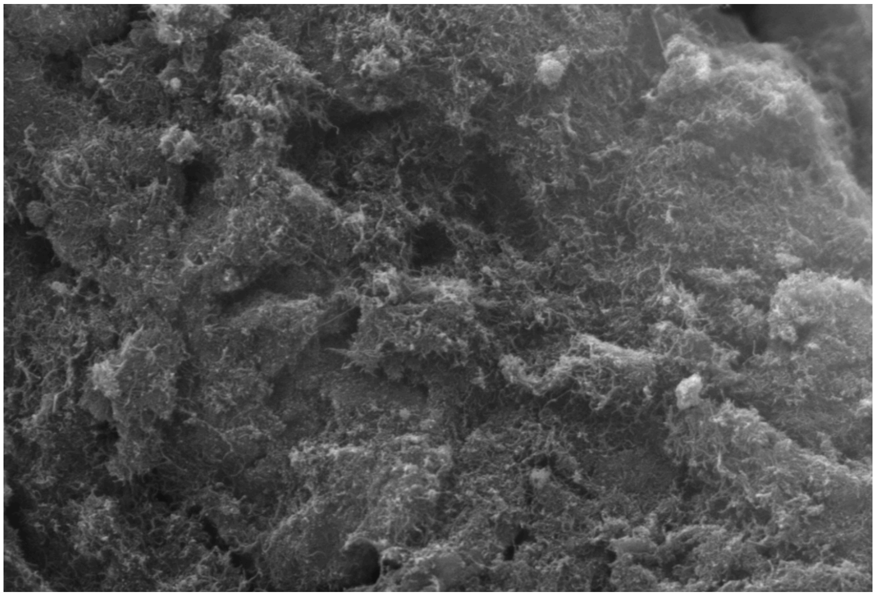

Fig 58 MWCNTs functionalized and seen through SEM.

The characterization of MWCNTs by XRD shows a characteristic diffraction plane between 25-30 (fig. 59) which denotes that once added to the Inconel 718 metal phase, it should be seen.

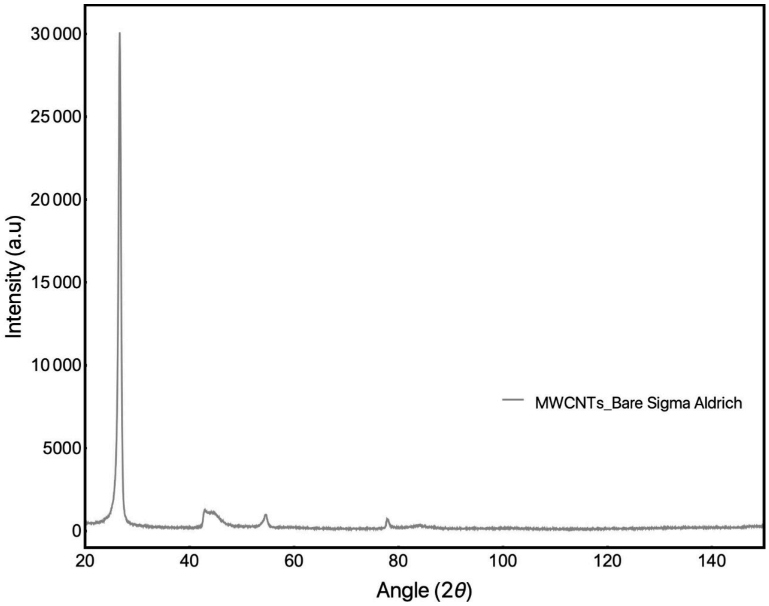

Fig 59 MWCNTs functionalized and seen through XRD.

The industrial grade MWCNTs which were used for these experiments, show different bands due to the processes by which they were carried. However, it can be seen that in the non-functionalized as in the functionalized (fig. 60) there are bands between 1700-1750, but the significant replica between 3200-3500 only occurs in the functionalized MWCNTs. This denotes that there was a change in its composition of functional groups, which were carbonyl groups.

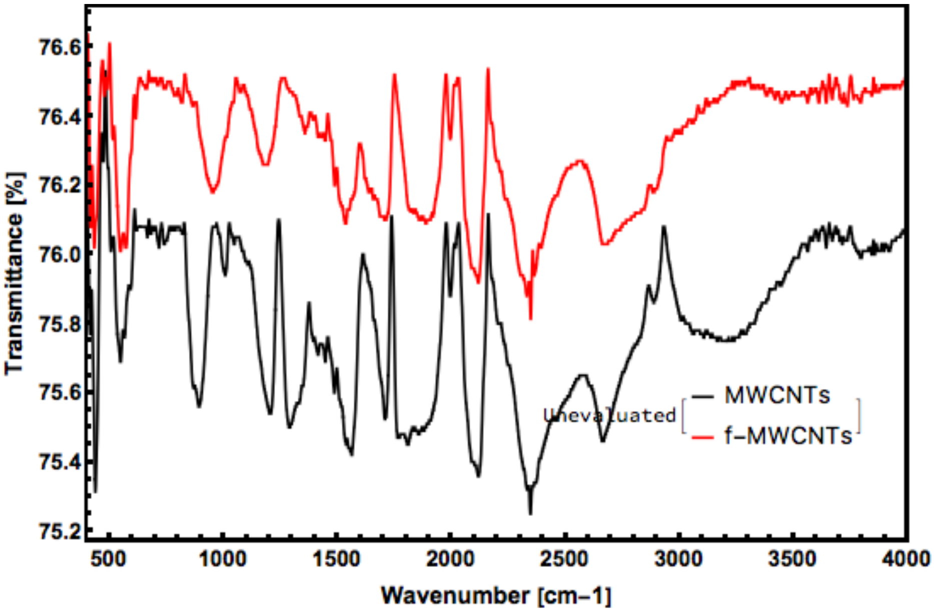

Fig 60 MWCNTs functionalized and seen through FTIR.

4.4 Adhesion of MWCNTs in Inconel 718

4.4.1 Inconel 718 Semi-Spherical

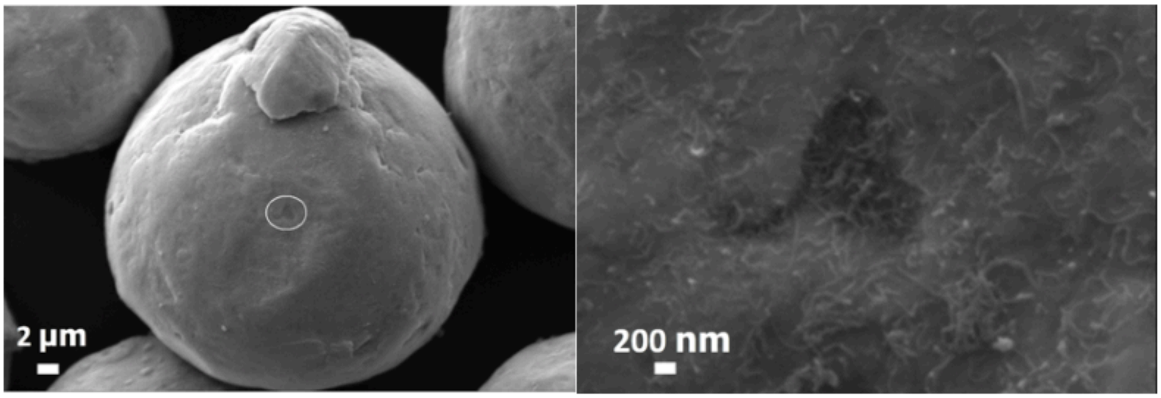

Fig 61 Semi-spherical morphology with MWNCTs by SEM.

Once the MWCNTs were added to the Inconel 718 metal matrix, it was characterized by SEM to be able to appreciate the MWCNTs, since this characterization technique allows increasing the magnification to see them. Once the images are obtained, it can be seen that at any point in the particle the magnification is increased, the presence of the MWCNTs can be seen (fig. 61). The agglomeration is nil or practically very little, since a very good dispersion was found in these images.

Based on the hypothesis that there would be an adhesion of the MWCNTs to the surface of Inconel 718, a characterization was made by means of XRD. Which resulted in the carbon phase of the MWCNTs being present. This is due to the fact that such diffraction plane is between 25-30, being reflected in the characterization (fig. 62).

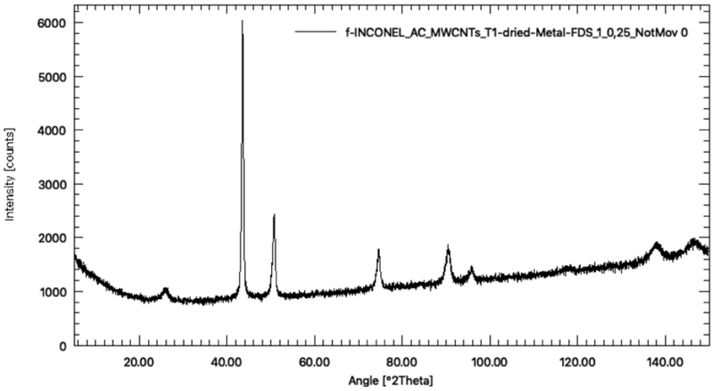

Fig 62 Semi-spherical morphology with MWNCTs by XRD.

4.4.2 Inconel 718 Flake

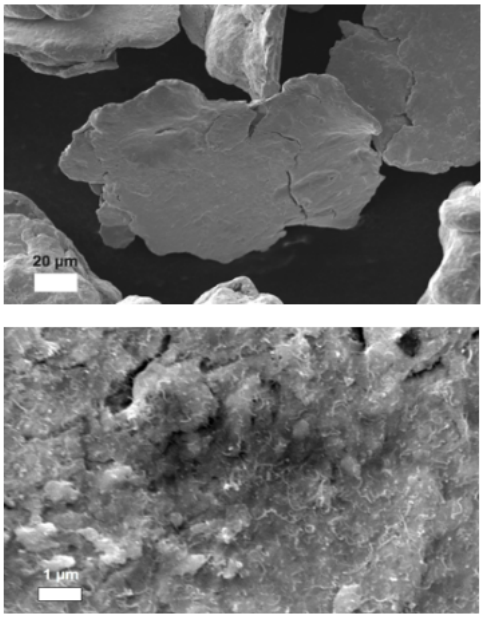

Fig 63 Flake morphology with MWNCTs by SEM.

The adhesion of the MWCNTs in the particles with flake morphology was carried out as with the semi-spherical particles. From SEM images (fig.63) it can be seen that there was a good dispersion of MWCNTs on the surface of the particle. Also, it can be seen that at any point in the particle studied, it will have MWCNTs, this indicates that the entire particle with this morphology was covered by the MWCNTs.

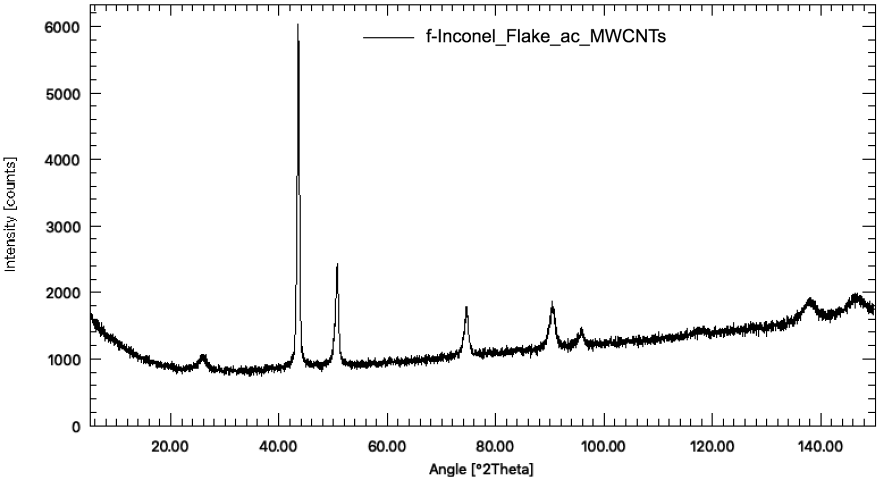

Fig 64 Flake morphology with MWNCTs by XRD.

Once the characterization is done through XRD, it is well known that the adhesion of the MWCNTs was made. This is because the diffraction plane between 25-30 was present (fig. 64). As in the semi-spherical particles the adhesion was carried out and through the characterization of XRD it was checked.

It is important to emphasize that the adhesion in each of these particles was carried out under the same conditions, with the same parameters in order to be able to make the punctual check under the different characterizations. Proving that adhesion works for both options and both are viable for possible use and future research.

5 Chapter 5: Conclusions

5.1 Conclusions

Once the nanocomposite of nickel superalloy with MWNCT has been created, it is concluded that:

The initial morphology of nickel superalloy was modified, resulting in two morphologies: hemispheric and scales. Subsequently, the functionalization processes were performed for the two resulting morphologies. The functionalization of MWCNT through acids introduced defects that produced carboxyl groups, with hydroxyls on the nanotube walls as an important point. The functionalization of the metal matrix through citric acid covered the particle so that once covered an affinity was created to join the MWCNT on the surface. Also, the characterization by SEM showed a visible binding of the MWNCT to the metal matrix. The XRD characterization showed a diffraction plane between 25-30 indicating that the carbon phase is present due to MWCNT.

The characterization by FTIR showed bands between 1700-1750 and 3250 that indicate the presence of carboxyl groups, indicating that the functionalization was effective and was achieved. SEM can see the distribution and adhesion of MWCNT to the metal matrix, however, no evidence was made to prove the effective distribution. The adhesion of the MWNCT is a fact. It is concluded that this nanocomposite can be used to create a piece and start with mechanical, electrical, thermal tests, among others, to verify a change in the physicochemical properties with the consolidated nanocomposite.

References

[1] Mrazova, M. (2013). Advanced composite materials of the future in aerospace industry. Incas bulletin, 5(3), 139.

[2] Jortner, J., & Rao, C. N. R. (2002). Nanostructured advanced materials. Perspectives and directions. Pure and applied chemistry, 74(9), 1491-1506.

[3] Smallman, R. E., & Ngan, A. H. W. (2011). Physical metallurgy and advanced materials. Elsevier.

[4] Yvon, P., & Carré, F. (2009). Structural materials challenges for advanced reactor systems. Journal of Nuclear Materials, 385(2), 217-222.

[5] Jaw, L. C. (2005, January). Recent advancements in aircraft engine health management (EHM) technologies and recommendations for the next step. In ASME turbo expo 2005: power for land, sea, and air (pp. 683-695). American Society of Mechanical Engineers.

[6] Dorji, U., & Ghomashchi, R. (2014). Hydro turbine failure mechanisms: An overview. Engineering Failure Analysis, 44, 136-147.

[7] Ruiz-Navas, E. M., da Costa, C. E., López, F. V., & Castelló, J. M. T. (2000). Mechanical alloy: Method of obtaining metal powders and composite materials. Metallurgy Magazine, 36 (4), 279-286.

[8] Kawamura, Y., Inoue, A., & Masumoto, T. (1993). Mechanical properties of amorphous alloy compacts prepared by a closed processing system. Scripta Metallurgica et Materialia;(United States), 29(1).

[9] Edris, H., McCartney, D. G., & Sturgeon, A. J. (1997). Microstructural characterization of high velocity oxy-fuel sprayed coatings of Inconel 625. Journal of materials science, 32(4), 863-872.

[10] Campbell, T. A., & Ivanova, O. S. (2013). 3D printing of multifunctional nanocomposites. Nano Today, 8(2), 119-120.

[11] Seetharaman, S. (2013). Treatise on process metallurgy, volume 3: industrial processes (Vol. 3). Newnes.

[12] Yefimov, N. A., & Naboychenko, S. (2009). Handbook of non-ferrous metal powders: technologies and applications. Elsevier.

[13] Yu, Y., Chen, Z., Wei, L., & Wang, B. (2017). The low-carbon technology characteristics of China's ferrous metal industry. Journal of cleaner production, 140, 1739-1748.

[14] Borzillo, A. R., & Horton, J. B. (1967). U.S. Patent No. 3,343,930. Washington, DC: U.S. Patent and Trademark Office.

[15] Elliott, R. (1988). Cast iron technology. Butterworth-Heinemann.

[16] Wang, H. X., & Li, Z. B. (2006). Application of microwave in ferrous metallurgy. Gangtie Yanjiu (Research on Iron and Steel), 34(4), 59-62.

[17] Angus, H. T. (2013). Cast iron: physical and engineering properties. Elsevier.

[18] Soroushian, P., & Choi, K. B. (1987). Steel mechanical properties at different strain rates. Journal of Structural Engineering, 113(4), 663-672.

[19] Hodgson, P. D., Hickson, M. R., & Gibbs, R. K. (2000). Ultrafine ferrite in low carbon steel. scripta Materialia, 40(10).

[20] Rabiei, A., Mumm, D. R., Hutchinson, J. W., Schweinfest, R., Rühle, M., & Evans, A. G. (2000). Microstructure, deformation and cracking characteristics of thermal spray ferrous coatings. Materials Science and Engineering: A, 269(1-2), 152-165.

[21] Berns, H., & Theisen, W. (2008). Ferrous materials: steel and cast iron. Springer Science & Business Media.

[22] Touloukian, Y. S., & Ho, C. Y. (Eds.). (1981). Properties of selected ferrous alloying elements (pp. 102-104). New York: McGraw-Hill.

[23] Beiss, P. (2003). Nonferrous materials. In Powder Metallurgy Data (pp. 460-470). Springer, Berlin, Heidelberg.

[24] Zhixin, M., Jie, H., Defu, L., & Yanli, L. (2003). Overview of Research and Manufacture of Layer-Metal Composite Plate [J]. Chinese Journal of Rare Metals, 6.

[25] Mondolfo, L. F. (2013). Aluminum alloys: structure and properties. Elsevier.

[26] Davis, J. R. (Ed.). (2001). Copper and copper alloys. ASM international.

[27] Davis, J. R. (Ed.). (2000). Nickel, cobalt, and their alloys. ASM international.

[28] Sudagar, J., Lian, J., & Sha, W. (2013). Electroless nickel, alloy, composite and nano coatings–A critical review. Journal of alloys and compounds, 571, 183-204.

[29] Hetmańczyk, M., Swadźba, L., & Mendala, B. (2007). Advanced materials and protective coatings in aero-engines application. Journal of Achievements in Materials and Manufacturing Engineering, 24(1), 372-381.

[30] Saito, Y., Önay, B., & Maruyama, T. (Eds.). (2012). High temperature corrosion of advanced materials and protective coatings. Elsevier.

[31] Thomas, M., Murray, S., & Furrer, D. (2010, October). Introducing new materials into aero engines—risks and rewards, a user's perspective. In 7th international symposium on superalloy (Vol. 718, pp. 3-11).

[32] Estrada, C. A. (2007). New technology used in gas turbine blade materials. Scientia et technica, 1(36).

[33] Herda, W. R., & Agarwal, D. C. (1999). Evolutionary development in nickel alloys and stainless-steel metallurgy for meeting the industry's corrosive challenges: the last 50 years. In Associazione Italiana di Metallurgia, (Vol. 2, pp. 117-125).

[34] Slama, C., & Abdellaoui, M. (2000). Structural characterization of the aged Inconel 718. Journal of alloys and compounds, 306(1-2), 277-284.

[35] Henderson, M. B., Arrell, D., Larsson, R., Heobel, M., & Marchant, G. (2004). Nickel based superalloy welding practices for industrial gas turbine applications. Science and technology of welding and joining, 9(1), 13-21.

[36] Thomas, A., El-Wahabi, M., Cabrera, J. M., & Prado, J. M. (2006). High temperature deformation of Inconel 718. Journal of materials processing technology, 177(1-3), 469-472.

[37] Jia, Q., & Gu, D. (2014). Selective laser melting additive manufacturing of Inconel 718 superalloy parts: Densification, microstructure and properties. Journal of Alloys and Compounds, 585, 713-721.

[38] Murr, L. E. (2015). Metallurgy of additive manufacturing: Examples from electron beam melting. Additive Manufacturing, 5, 40-53.

[39] Shen, G., & Furrer, D. (2000). Manufacturing of aerospace forgings. Journal of Materials Processing Technology, 98(2), 189-195.

[40] De la Rosa Blanco, E., Hall, C., & Crichton, D. (2007, January). Challenges in the silent aircraft engine design. In 45th AIAA aerospace sciences meeting and exhibit (p. 454).

[41] Levy, G. N., Schindel, R., & Kruth, J. P. (2003). Rapid manufacturing and rapid tooling with layer manufacturing (LM) technologies, state of the art and future perspectives. CIRP annals, 52(2), 589-609.

[42] Yap, C. Y., Chua, C. K., Dong, Z. L., Liu, Z. H., Zhang, D. Q., Loh, L. E., & Sing, S. L. (2015). Review of selective laser melting: Materials and applications. Applied physics reviews, 2(4), 041101.

[43] Liu, Z., & Qi, H. (2015). Effects of substrate crystallographic orientations on crystal growth and microstructure formation in laser powder deposition of nickel-based superalloy. Acta Materials, 87, 248-258.

[44] Liu, Z., & Qi, H. (2015). Effects of processing parameters on crystal growth and microstructure formation in laser powder deposition of single-crystal superalloy. Journal of Materials Processing Technology, 216, 19-27.

[45] Jiang, L., Fan, G., Li, Z., Kai, X., Zhang, D., Chen, Z., ... & Yeung, W. Y. (2011). An approach to the uniform dispersion of a high-volume fraction of carbon nanotubes in aluminum powder. Carbon, 49(6), 1965-1971.

[46] Kong, J., Yenilmez, E., Tombler, T. W., Kim, W., Dai, H., Laughlin, R. B., ... & Wu, S. Y. (2001). Quantum interference and ballistic transmission in nanotube electron waveguides. Physical review letters, 87(10), 106801.

[47] Frank, S., Poncharal, P., Wang, Z. L., & De Heer, W. A. (1998). Carbon nanotube quantum resistors. science, 280(5370), 1744-1746.

[48] Hjortstam, O., Isberg, P., Söderholm, S., & Dai, H. (2004). Can we achieve ultra-low resistivity in carbon nanotube-based metal composites? Applied Physics A, 78(8), 1175-1179.

[49] Pereira, J. M., & Lerch, B. A. (2001). Effects of heat treatment on the ballistic impact properties of Inconel 718 for jet engine fan containment applications. International Journal of Impact Engineering, 25(8), 715-733.

[50] Hirsch, A. (2010). The era of carbon allotropes. Nature materials, 9(11), 868.

[51] Ryu S-W, Huang X-J, Choi Y-K. Appl. Phys. Lett. 2007, 91, 063110-3.

[52] Azzellino G, Grimoldi a, Binda M, Caironi M, Natali D, Sampietro M. Adv. Mater. 2013, 25, 6829–6833.

[53] Bansal M, Srivastava R, Lal C, Kamalasanan MN, Tanwar LS. Int. J. Mod. Phys. B. 2011, 25, 2543–2556.

[54] Sleiman A, Mabrook MF, Nejm RR, et al. J. Appl. Phys. 2012, 112, 024509-5.

[55] Sleiman A, Rosamond MC, Alba Martin M, et al. Appl. Phys. Lett. 2012, 100, 023302-4.

[56] Verbakel, F. (2008). Resistive switching in polymer-metal oxide diodes for electronic memory applications.

[57] Raymo FM. Advanced Materials 2002, 14, 401-414.

[58] Reed MA, Zhou C. Muller CJ, et al. Science 1997, 278, 252-254.

[59] Yang Y, Ouyang J, Ma LP, et al. Advanced Functional Materials 2006, 16, 1001-1014.

[60] K Jiang, A Eitan, L. S. Schadler, P. M. Ajayan, R. W. Siegel. N. Grobert, M. Mayne, M. Reyes-Reyes, H. Terrones and M. Terrones. "Selective Attachment of Gold Nanoparticles to Nitrogen-Doped Carbon Nanotubes" Nano Lett. 3 (2003) 275.

[61] A. Rubio, J.L. Corkill, M.L. Cohen. "Theory of graphitic boron nitride nanotubes". Phys. Rev. B 49 (1994) 5081.

[62] Y. Miyamoto, A. Rubio, S.G. Louie, M.L. Cohen. "Electronic properties of tubule forms of hexagonal BC3". Phys. Rev. B 50 (1994) 18360.

[63] Shen, C., Brozena, A. H., & Wang, Y. (2011). Double-walled carbon nanotubes: challenges and opportunities. Nanoscale, 3(2), 503-518.

[64] Thostenson, E. T., Ren, Z., & Chou, T. W. (2001). Advances in the science and technology of carbon nanotubes and their composites: a review. Composites science and technology, 61(13), 1899-1912.

[65] Trojanowicz, M. (2006). Analytical applications of carbon nanotubes: a review. TrAC trends in analytical chemistry, 25(5), 480-489.

[66] Aqel, A., El-Nour, K. M. A., Ammar, R. A., & Al-Warthan, A. (2012). Carbon nanotubes, science and technology part (I) structure, synthesis and characterization. Arabian Journal of Chemistry, 5(1), 1-23.

[67] None. (1979). Powder Metallurgy in The Electronics Industry. Powder Metallurgy, 22(3), 145-153.

[68] Rael, B. (2016). Optimizing Powder Metallurgy Methods: Carbon Nanotube Metal Composites.

[69] Chen, M., Fan, G., Tan, Z., Xiong, D., Guo, Q., Su, Y., ... & Zhang, D. (2018). Design of an efficient flake powder metallurgy route to fabricate CNT/6061Al composites. Materials & Design, 142, 288-296.

[70] Zhang, L., Hou, G., Zhai, W., Ai, Q., Feng, J., Zhang, L., ... & Ci, L. (2018). Aluminum/graphene composites with enhanced heat-dissipation properties by in-situ

reduction of graphene oxide on aluminum particles. Journal of Alloys and Compounds, 748, 854-860.

[71] Esawi, A., & Morsi, K. (2007). Dispersion of carbon nanotubes (CNTs) in a metal powder. Composites Part A: Applied Science and Manufacturing, 38(2), 646-650.

[72] Fan, G., Jiang, Y., Tan, Z., Guo, Q., Xiong, D. B., Su, Y., ... & Zhang, D. (2018). Enhanced interfacial bonding and mechanical properties in CNT/Al composites fabricated by flake powder metallurgy. Carbon, 130, 333-339.

[73] Pal, S. K., Son, Y., Borca-Tasciuc, T., Borca-Tasciuc, D. A., Kar, S., Vajtai, R., & Ajayan, P. M. (2008). Thermal and electrical transport along MWCNT arrays grown on Inconel substrates. Journal of Materials Research, 23(8), 2099-2105.

[74] Wang, P., Zhang, B., Tan, C. C., Raghavan, S., Lim, Y. F., Sun, C. N., ... & Chi, D. (2016). Microstructural characteristics and mechanical properties of carbon nanotube reinforced Inconel 625 parts fabricated by selective laser melting. Materials & Design, 112, 290-299.

[75] Hegab, H., Umer, U., Soliman, M., & Kishawy, H. A. (2018). Effects of nano-cutting fluids on tool performance and chip morphology during machining Inconel 718. The International Journal of Advanced Manufacturing Technology, 96(9-12), 3449-3458.

[76] Lu, X. B., & Dai, J. Y. (2006). Memory effects of carbon nanotubes as charge storage nodes for floating gate memory applications. Applied physics letters, 88(11), 113104.

[77] Liu, G., Ling, Q. D., Teo, E. Y. H., Zhu, C. X., Chan, D. S. H., Neoh, K. G., & Kang, E. T. (2009). Electrical conductance tuning and bistable switching in poly (N-vinylcarbazole) − carbon nanotube composite films. ACS nano, 3(7), 1929-1937.

[78] Liu G, Ling QD, Kang E-T, et al. J. Appl. Phys. 2007, 102, 024502-8

[79] Chai, Y., Wu, Y., Takei, K., Chen, H. Y., Yu, S., Chan, P. C., ... & Wong, H. S. P. (2011). Nanoscale bipolar and complementary resistive switching memory based on amorphous carbon. IEEE transactions on electron devices, 58(11), 3933-3939.

[80] Cui JB, Sordan R, Burghard M, Kern K. Appl. Phys. Lett. 2002, 81, 3260-3264.

[81] Cava, C. E., Possagno, R., Schnitzler, M. C., Roman, P. C., Oliveira, M. M., Lepiensky, C. M., ... & Roman, L. S. (2007). Iron-and iron oxide-filled multi-walled carbon nanotubes: Electrical properties and memory devices. Chemical Physics Letters, 444(4-6), 304-308.

[82] Mamo, M. A., Machado, W. S., van Otterlo, W. A., Coville, N. J., & Hümmelgen, I. A. (2010). Simple write-once-read-many-times memory device based on a carbon sphere-poly (vinylphenol) composite. Organic Electronics, 11(11), 1858-1863.

[83] Möller, S., Forrest, S. R., Perlov, C., Jackson, W., & Taussig, C. (2003). Electrochromic conductive polymer fuses for hybrid organic/inorganic semiconductor memories. Journal of applied physics, 94(12), 7811-7819.

[84] Ha H, Kim O. Appl. Phys. Lett. 2008, 93, 033309-3.

[85] Liu, X., Ji, Z., Tu, D., Shang, L., Liu, J., Liu, M., & Xie, C. (2009). Organic nonpolar nonvolatile resistive switching in poly (3, 4-ethylene-dioxythiophene): Polystyrenesulfonate thin film. Organic Electronics, 10(6), 1191-1194.

[86] Yang J, Zeng F, Wang ZS, et al. J. Appl. Phys. 2001, 110, 114518-5.

[87] Zhang, S., Leem, G., Srisombat, L. O., & Lee, T. R. (2008). Rationally designed ligands that inhibit the aggregation of large gold nanoparticles in solution. Journal of the American Chemical Society, 130(1), 113-120.

[88] Riaz, S., Naseem, S., & Han, X. (2015, May). Citric acid coated iron oxide nanoparticles—Structural and magnetic properties. In 2015 IEEE International Magnetics Conference (INTERMAG) (pp. 1-1). IEEE.

[89] G. Goloverda, B. Jackson, C. Kidd, V. Kolesnichenko, "Synthesis of ultrasmall magnetic iron oxide nanoparticles and study of their colloid and surface chemistry," J. Magn. Magn. Mater., vol. 321, pp. 1372–1376, 2009.

[90] B. Behdadfar, A. Kermanpur, H. S. Aliabadi, M. P. Morales, and M. Mozaffari, "Synthesis of high intrinsic loss power aqueous ferrofluids of iron oxide nanoparticles by citric acid assisted hydrothermal-reduction route," J. Solid State Chem., vol. 187, pp. 20–26, 2012.

[91] L. Li, K. Y. Mak, C. W. Leung, K. Y. Chan, W. K. Chan, W. Zhong, and P. W. T. Pong, "Effect of synthesis conditions on the properties of citric-acid coated iron oxide nanoparticles," Microelectron. Eng., vol. http://dx.doi.org/10.1016/j.mee.2013.02.045, 2013.

[92] Bishop, L. M., Yeager, J. C., Chen, X., Wheeler, J. N., Torelli, M. D., Benson, M. C., ... & Hamers, R. J. (2011). A citric acid-derived ligand for modular functionalization of metal oxide surfaces via "click" chemistry. Langmuir, 28(2), 1322-1329.

[93] Kralj, S., Makovec, D., Čampelj, S., & Drofenik, M. (2010). Producing ultra-thin silica coatings on iron-oxide nanoparticles to improve their surface reactivity. Journal of Magnetism and Magnetic Materials, 322(13), 1847-1853.

[94] Hsin, Y. L., Lai, J. Y., Hwang, K. C., Lo, S. C., Chen, F. R., & Kai, J. J. (2006). Rapid surface functionalization of iron-filled multi-walled carbon nanotubes. Carbon, 44(15), 3328-3335.
[95] Jeon, S., Kim, J., & Kim, K. H. (2019). Microwave absorption properties of graphene oxide capsulated carbonyl iron particles. Applied Surface Science, 475, 1065-1069.

[96] Koch, C. C. (1997). Synthesis of nanostructured materials by mechanical milling: problems and opportunities. Nanostructured Materials, 9(1-8), 13-22.

[97] Suryanarayana, C. (2001). Mechanical alloying and milling. Progress in materials science, 46(1-2), 1-184.

[98] Zhao, X., Ding, Y., Ma, L., Shen, X., & Xu, S. (2008). Structure, morphology and electrocatalytic characteristics of nickel powders treated by mechanical milling. international journal of hydrogen energy, 33(21), 6351-6356.

[99] Bakshi, S. R., Lahiri, D., & Agarwal, A. (2010). Carbon nanotube reinforced metal matrix composites-a review. International materials reviews, 55(1), 41-64.

[100] Esawi, A., & Morsi, K. (2007). Dispersion of carbon nanotubes (CNTs) in aluminum powder. Composites Part A: Applied Science and Manufacturing, 38(2), 646-650.

[101] Bakshi, S. R., Singh, V., Seal, S., & Agarwal, A. (2009). Metal composites reinforced with multiwalled carbon nanotubes from plasma spraying of spray dried powders. Surface and Coatings Technology, 203(10-11), 1544-1554.